CellPress
Partner Journal

Molecular Plant
Research Article

Redox sensor QSOX1 regulates plant immunity by targeting GSNOR to modulate ROS generation

Ho Byoung Chae[1,8], Min Gab Kim[2,8], Chang Ho Kang[1], Joung Hun Park[1], Eun Seon Lee[1], Sang-Uk Lee[3], Yong Hun Chi[7], Seol Ki Paeng[1], Su Bin Bae[1], Seong Dong Wi[1], Byung-Wook Yun[3], Woe-Yeon Kim[1], Dae-Jin Yun[4], David Mackey[5,*] and Sang Yeol Lee[1,6,*]

[1]Division of Applied Life Sciences (BK21) and PMBBRC, Gyeongsang National University, Jinju 52828, Korea

[2]College of Pharmacy, Research Institute of Pharmaceutical Science, Gyeongsang National University, Jinju 52828, Korea

[3]School of Applied Biosciences, College of Agriculture and Life Sciences, Kyungpook National University, Daegu 41566, Korea

[4]Department of Biomedical Science and Engineering, Konkuk University, Seoul 05029, Korea

[5]Department of Horticulture and Crop Science, Department of Molecular Genetics, and Center for Applied Plant Sciences, The Ohio State University, Columbus, OH 43210, USA

[6]College of Life Sciences, Qingdao Agricultural University, Qingdao 266109, P.R. China

[7]Plant Propagation Team, Plant Production Division, Sejong National Arboretum, Sejong 30106, Korea

[8]These authors contributed equally

***Correspondence: David Mackey (mackey.86@osu.edu), Sang Yeol Lee (sylee@gnu.ac.kr)**

https://doi.org/10.1016/j.molp.2021.05.004

ABSTRACT

Reactive oxygen signaling regulates numerous biological processes, including stress responses in plants. Redox sensors transduce reactive oxygen signals into cellular responses. Here, we present biochemical evidence that a plant quiescin sulfhydryl oxidase homolog (QSOX1) is a redox sensor that negatively regulates plant immunity against a bacterial pathogen. The expression level of *QSOX1* is inversely correlated with pathogen-induced reactive oxygen species (ROS) accumulation. Interestingly, QSOX1 both senses and regulates ROS levels by interactingn with and mediating redox regulation of S-nitrosoglutathione reductase, which, consistent with previous findings, influences reactive nitrogen-mediated regulation of ROS generation. Collectively, our data indicate that QSOX1 is a redox sensor that negatively regulates plant immunity by linking reactive oxygen and reactive nitrogen signaling to limit ROS production.

Key words: redox sensor, plant immunity, QSOX1, GSNOR, reactive oxygen species (ROS), reactive nitrogen species (RNS)

Chae H.B., Kim M.G., Kang C.H., Park J.H., Lee E.S., Lee S.-U., Chi Y.H., Paeng S.K., Bae S.B., Wi S.D., Yun B.-W., Kim W.-Y., Yun D.-J., Mackey D., and Lee S.Y. (2021). Redox sensor QSOX1 regulates plant immunity by targeting GSNOR to modulate ROS generation. Mol. Plant. **14**, 1312–1327.

INTRODUCTION

Reactive oxygen species (ROS) produced constantly as byproducts of photosynthesis and aerobic metabolism are also rapidly induced signaling molecules. However, persistently high levels of ROS damage intracellular biological components leading to inflammatory and degenerative diseases (Wiseman and Halliwell, 1996; Trachootham et al., 2009). Cells must therefore balance the transient induction of ROS for cellular responses with restoring homeostasis to limit its detrimental effects. Precise control of ROS production and scavenging, as well as ROS signaling, rely on reversibly oxidized sensor proteins that transduce changes in redox potential into diverse signaling pathways through oxidative modifications of themselves and client molecules, including a variety of thiol-based redox proteins (Foyer and Noctor, 2005; Veal et al., 2007; Garcia-Santamarina et al., 2014; Hillion and Antelmann, 2015; Liu and He, 2016).

The ability of cells to regulate both production and elimination of ROS, as well as to transduce ROS-induced signaling, relies on redox sensor proteins that are oxidized and reduced reversibly in response to ROS levels. Several thiol-based redox proteins with low pK_a values, including protein tyrosine phosphatases (PTSs) and glyceraldehyde-3-phosphate dehydrogenase (GAPDH), have been identified as redox sensors that finely tune the intracellular responses to changes in the level of ROS (Veal et al., 2007; Ostman et al., 2011; Tristan et al., 2011; Garcia-Santamarina et al., 2014). Acting as molecular switches, redox sensors respond to changes in redox potential through oxidative modifications of residues on both themselves and client molecules, such as the formation of disulfide bonds (RSSR), sulfenation (SOH), sulfination (SO_2H),

Published by the Molecular Plant Shanghai Editorial Office in association with Cell Press, an imprint of Elsevier Inc., on behalf of CSPB and CEMPS, CAS.

sulfonation (SO_3H), S-nitrosylation (RSNO), peroxynitration (R-O NOO), and glutathionylation (RSSG) (Spadaro et al., 2010). These post-translational modifications transduce redox-mediated stimuli into diverse signaling pathways for the regulation of downstream gene transcription, translation, protein folding and stability, and subcellular localization of biological molecules (Jang et al., 2004). Redox-regulated oxidation/reduction of regulatory or active site thiols modifies the activity of various classes of proteins, including kinases, proteases, transcription factors and co-factors, disulfide bond family proteins, protein disulfide isomerases (PDIs) and other oxidoreductases belonging to the thioredoxin (Trx), glutaredoxin, or peroxiredoxin subfamilies (Vazquez-Torres, 2012; Chae et al., 2013; Hillion and Antelmann, 2015).

Plants lead a sessile lifestyle during which they encounter numerous biotic and abiotic stresses. A hallmark response is a burst of ROS, frequently generated by the respiratory burst NADPH oxidase homologs (RBOHs) located in the plant plasma membrane (Grant and Loake, 2000; Torres et al., 2002; Foreman et al., 2003; Kwak et al., 2003). RBOH-produced ROS functions prominently in the plant immune system, including basal defense and effector-triggered immunity (ETI) resulting from activation of NOD-like receptors (NLRs) that typically have C-terminal Toll/interleukin-1 (TNL) or coiled-coil (CNL) domains (Gomez-Gomez and Boller, 2000; Schwessinger and Ronald, 2012; Zipfel, 2014). RBOH-produced ROS regulates defense-associated cell death, termed the hypersensitive response (HR), which is frequently induced during ETI (Torres et al., 2002; Jones and Dangl, 2006; Torres, 2010; Jwa and Hwang, 2017). Both basal defense and CNL- or TNL-induced ETI result in elevated levels of salicylic acid (SA), which is part of a feedforward loop for ROS production (Herrera-Vasquez et al., 2015). In addition, SA promotes ROS scavenging, at least in part through increased glutathione levels and reducing power, by a currently unknown mechanism (Mou et al., 2003; Mateo et al., 2006). Prominent transcriptional reprogramming associated with SA-signaling results from redox-mediated changes in the oligomerization state, subcellular localization, and post-translational modification of non-expressor of PR1 (NPR1) (Mou et al., 2003; Tada et al., 2008; Lindermayr et al., 2010). Redox status has also been implicated in regulating TGA transcription factors, which functionally associate with NPR1, and jasmonic acid (JA) signaling, which is often antagonistic to SA signaling (Mur et al., 2006; Leon-Reyes et al., 2010; Farmer and Mueller, 2013). While a rapid ROS burst is essential for robust and timely responses to biotic stress, over- or mis-regulated accumulation of ROS is detrimental. Plants displaying hybrid incompatibility, as well as mutant plants identified in genetic screens, such as those for ‘‘constitutive expression of PR1’’ and ‘‘accelerated cell death,’’ have elevated levels of ROS and reduced stature, associated with expression of defense genes and HR-like cell death (Todesco et al., 2010; Chae et al., 2014; Zhu et al., 2018). Thus, homeostatic control of ROS levels is critical to effective plant immunity without inappropriately activated or constitutive defense responses detrimental to plant growth and productivity (Chugh et al., 2011).

Identification of novel redox sensors, which regulate global networks of diverse metabolic pathways and thus crucial functions in cellular processes, is of great interest. However, theoretical predictions based on Cys residues has proven challenging (Weerapana et al., 2010). To identify redox sensors in the model plant *Arabidopsis*, we searched redox proteins from the http://www.arabidopsis.org/ database and found a strong candidate with homology to mammalian quiescin sulfhydryl oxidase (QSOX), so named for its induction at the quiescent stages of human fibroblast cells (Thorpe et al., 2002). QSOX contains two discrete redox-active domains; a PDI-like oxidoreductase with an active CxxC motif within a Trx-like fold and a sulfhydryl oxidase mitochondrial ERV/ALR-related domain with two CxxC motifs and a flavin adenine dinucleotide (FAD)-binding motif. The lower predicted pK_a of the Trx domain, coupled with the capacity for efficient transfer of electrons via a dithiol/disulfide relay to the EVR/ALR domain, then to FAD, and ultimately to terminal electron acceptors, uniquely suits QSOX to sense ROS accumulation and tune the oxidation state of client substrates during a variety of biological processes (Thorpe et al., 2002; Alon et al., 2012). Mammalian QSOX, which regulates protein folding and stability of matrix proteins by exchanging the intermolecular dithiol/disulfide bridges of target substrates (Ilani et al., 2013), functions in various subcellular organelles, including extracellular secretory granules, mitochondria, the Golgi complex, and the endoplasmic reticulum, to regulate oxidative stress-mediated liver degeneration, neuroblastoma tumorigenesis, prevention of angiogenesis, apoptosis, cancer, and degenerative diseases (Benayoun et al., 2001; Katchman et al., 2011; Margittai and Sitia, 2011; Pernodet et al., 2012; Das et al., 2013; Ilani et al., 2013; Shi et al., 2013; Poillet et al., 2014). Despite the functional importance of mammalian QSOX proteins, the limited knowledge about plant QSOX proteins prompted us to investigate the two homologs of QSOX in *Arabidopsis*, AtQSOX1 and AtQSOX2 (Alejandro et al., 2007).

Induced expression following pathogen challenge or exposure to plant defense hormones focused our efforts on *AtQSOX1*. Through knockout and overexpression, we demonstrate that *AtQSOX1* negatively regulates ROS levels following an initial ROS burst induced during plant immunity. Consistent with this finding, elimination or overexpression of *AtQSOX1* heightens or dampens, respectively, resistance against both virulent and avirulent pathogens. AtQSOX1, which we demonstrate to possess oxidoreductase activity, regulates ROS levels, at least in part, through interacting with and oxidizing AtGSNOR. The AtQSOX1-mediated oxidative inactivation of GSNOR elevates intracellular levels of GSNO, which limits further ROS production through inhibition of RBOHs (Yun et al., 2011). These results reveal a mechanism through which plants sense an immune-associated increase in ROS and subsequently favor restoration of redox homeostasis via crosstalk with reactive nitrogen signaling to limit the ongoing production of ROS.

RESULTS

Expression of *AtQSOX1* is regulated during plant immune responses

Based on the hypothesized function of AtQSOX proteins as redox sensors and the known role of ROS during plant immunity, we tested accumulation of the *AtQSOX1* and *AtQSOX2* (hereafter *QSOX1* and *QSOX2*) transcripts following a variety of stresses. Abundance of *QSOX1* transcripts, measured by RT–PCR, were unaffected by cold, heat, and methyl viologen-induced oxidative stress (Figure 1A). However, unlike *QSOX2*,

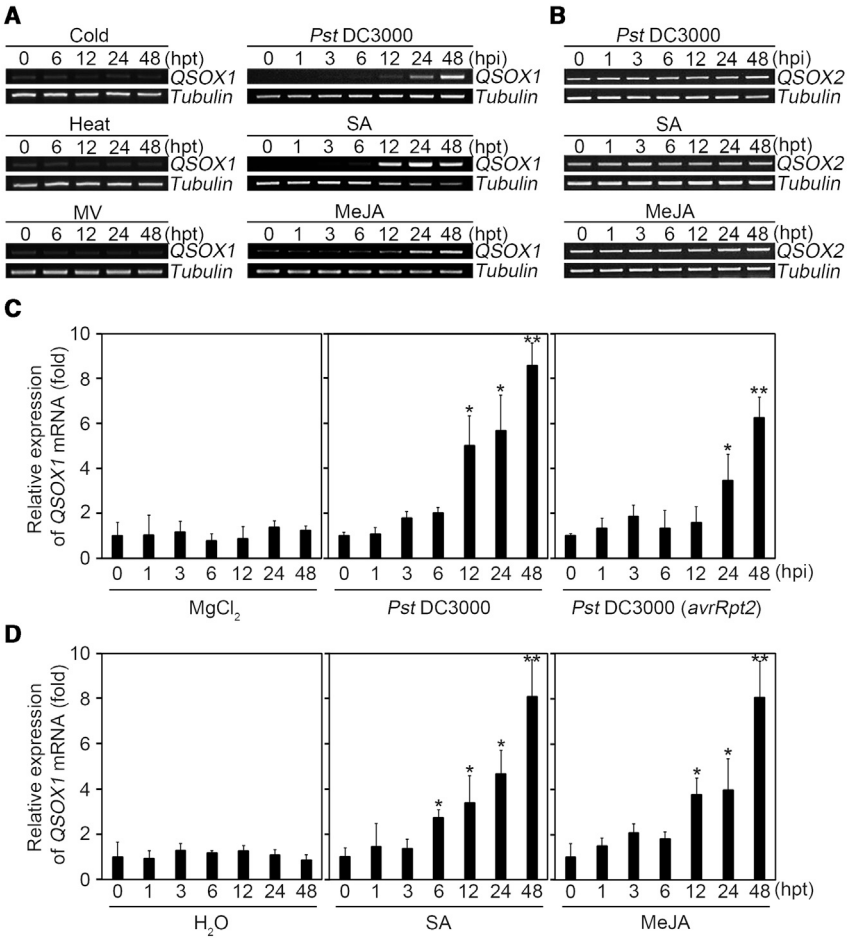

Figure 1. QSOX1 is involved in plant immune response.

(A) RT–PCR analysis of *QSOX1* expression using 2-week-old wild-type plants under various biotic and abiotic stresses. Plants were vacuum infiltrated with 10^8 cfu/ml *Pst* DC3000, 2 mM SA, 100 μM MeJA, 5 μM methyl viologen (MV), or exposed to 4°C cold or 37°C heat and samples were harvested at the indicated time points, hours post treatment (hpt). A *tubulin* gene was used as a loading control.

(B) RT–PCR analysis of *QSOX2* expression in wild-type plants under various stresses. Two-week-old plants, grown on plates of ½ MS salt with 2% sucrose (pH 5.8), were vacuum infiltrated with 10^8 cfu/ml *Pst* DC3000, 2 mM SA, or 100 μM MeJA. Samples were harvested at the times indicated for RT–PCR analysis.

(C and D) Quantitative real-time PCR analysis of *QSOX1* expression using 2-week-old wild-type plants. Statistical significance of the experiments was analyzed by Student's *t*-test compared with time zero (*$P < 0.05$, **$P < 0.01$). Expression of *QSOX1* in plants after inoculation of a control solution (10 mM $MgCl_2$), 10^8 cfu/ml of *Pst* DC3000, or *Pst* DC3000 (*avrRpt2*) **(C)**. Expression of *QSOX1* in plants after vacuum infiltration of a water control, 2 mM SA, or 100 μM MeJA **(D)**.

See also Supplemental Table 1.

QSOX1 was induced by various biotic stresses, including challenge with the virulent, Gram-negative bacterial pathogen *Pseudomonas syringae* pv. *tomato* DC3000 (*Pst* DC3000), an avirulent strain of *Pst* DC3000 carrying a plasmid expressing the ETI-eliciting type III effector AvrRpt2 (*Pst* DC3000 [*avrRpt2*]), as well as the defense hormones SA and methyl jasmonate (MeJA), which is a precursor to biologically active JA. Because *Pst* DC3000, SA, or MeJA had no effect on transcript levels of *QSOX2* (Figure 1B), we conducted a more thorough qRT–PCR analyses of *QSOX1* expression (Figure 1C and 1D). *Pst* DC3000 caused a significant increase in *QSOX1* transcript levels by 12 h after infiltration with a continuing increase until at least 48 h. *Pst* DC3000 (*avrRpt2*) also induced significant accumulation of *QSOX1* transcripts, although with slower kinetics and reduced magnitude, possibly due to cell death resulting from the induced HR. Vacuum infiltration with SA and MeJA each significantly increased *QSOX1* transcript levels by 6 and 12 h, respectively, and for at least 48 h.

Oxidoreductase activity of QSOX1

Oxidoreductase activity has been demonstrated for a plant QSOX from soybean (GmQSOX1) (Okuda et al., 2014). To determine if QSOX1 (Figure 2A) could similarly oxidize a protein substrate *in vitro*, we purified it to near homogeneity from *E. coli* (Supplemental Figure 1). Contrary to previous findings (Limor-Waisberg et al., 2012), recombinant QSOX1 oxidized nearly all of reduced RNase A during a 2 h incubation, as measured by increased mobility of oxidized RNase A in non-reducing SDS–PAGE (Figure 2B). The rate of RNase A oxidation was increased by addition of a 10-fold excess of FAD relative to QSOX1 (Figure 2C), and substrate oxidation after 30 min was correlated with increasing concentrations of FAD (Figure 2D), indicating that FAD molecules likely serve as terminal electron acceptors during the oxidization of RNase A by QSOX1.

QSOX1 contains redox-active disulfide pairs in both its Trx and ERV/ALR domains. The contribution of the reactive cysteines within each of these domains to oxidation of the RNase A substrate was determined (Figure 2E). Recombinant proteins with the active cysteines of the Trx domain (QSOX1-M1), the ERV/ALR domain (QSOX1-M2), or both (QSOX1-M3), mutated to serines (Supplemental Figure 1A) were purified to near homogeneity (Supplemental Figure 1B). QSOX1-M3 does not detectably oxidize RNase A, as predicted. QSOX1 and QSOX1-M1 each oxidize RNase A at a similar rate while QSOX1-M2 oxidizes RNase A at a reduced rate relative to QSOX1, likely due to the combined effect of the molar excess of RNase A to QSOX1-M2 and its inability to relay electrons from the Trx domain to the mutated cysteines of the ERV/ALR domain. Thus, although the reactive cysteines within the Trx and ERV/ALR domains each have the capacity to receive electron from reduced RNase A, under our reaction conditions, the ERV/ALR domain efficiently, directly oxidizes RNase A and transfer of electrons from the cysteines of the ERV/ALR domain to FAD is the rate-limiting step in the reaction.

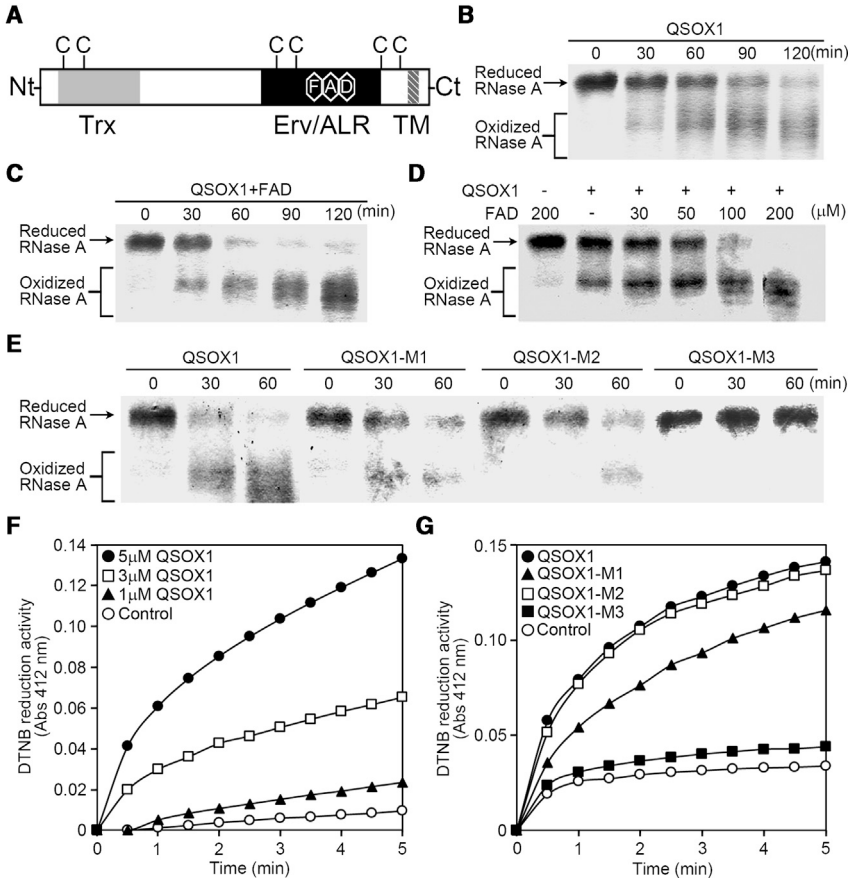

Figure 2. QSOX1 is an active oxidoreductase.
(A) Primary protein structure of QSOX1. Position of CxxC motifs and the FAD binding site within Trx (gray) and ERV/ALR (black) domains are indicated.
(B and C) Oxidation of reduced RNase A (20 μM) by QSOX1 (3 μM) in the absence **(B)** or presence of 30 μM FAD **(C)**.
(D) Oxidation of reduced RNase A by QSOX1 (3 μM) after 30 min in the presence of different concentrations of FAD.
(E) Oxidation of reduced RNase A by QSOX1 and its M1, M2, and M3 derivatives (3 μM).
(F) Reduction of DTNB (5 mM) without (○) or with 1 (▲), 3 (□), or 5 (●) μM of QSOX1.
(G) Reduction of DTNB without (○) or with QSOX1 (●) or its M1 (▲), M2 (□), and M3 (■) derivatives (5 μM).
See also Supplemental Figure 1 and Supplemental Table 1.

The ability of wild-type and M1, M2, and M3 mutant versions of QSOX1 proteins to reduce a test substrate, 5,5′-dithiobis-(2-nitrobenzoic acid) (DTNB), *in vitro* was measured. Incubation of increasing concentrations of QSOX1 with a ≥1000-fold molar excess of DTNB showed a dose-dependent increase in reduction of the test substrate (Figure 2F). QSOX1 and QSOX1-M2 reduced DTNB at equal rates, while QSOX1-M1 showed a reduced rate and QSOX1-M3 scarcely differed from the control reaction (Figure 2G). These results indicate that reactive cysteines of both the Trx and ERV/ALR domains can serve as electron donors and that, consistent with their predicted lower pK_a, the reactive cysteines of the Trx domain do so more efficiently under our reaction conditions (Thorpe et al., 2002).

QSOX1 negatively regulates plant immunity against *P. syringae*

The induction of QSOX1 by bacterial pathogens and immune-associated hormones, coupled with its ability to relay electrons from a substrate to the reactive cysteines of relatively lower pK_a in its Trx domain, then to reactive cysteines of relatively higher pK_a in its ERV/ALR domain, and ultimately to FAD, led us to hypothesize that it is a redox sensor that functions in plant immunity. To test this hypothesis, we identified *Arabidopsis* plants with T-DNA insertions predicted to disrupt *QSOX1* (AT1G15020) and *QSOX2* (AT2G01270). Homozygous lines were identified and RT–PCR failed to detect the full-length transcripts (Supplemental Figure 2A and 2B). Spray inoculation of these mutants, designated as *qsox1* (previously referred to as *par1-4* [Alejandro et al., 2007]) and *qsox2*, with *Pst* DC3000, revealed that *qsox1* plants showed reduced disease symptoms and bacterial growth (Figure 3A and 3B). The lack of an apparent pathology phenotype for *qsox2*, together with the observation that expression of *QSOX2* is not regulated during biotic stress responses (Figure 1B), led us to focus subsequent studies on the putative negative regulator of plant immunity, *QSOX1*.

To confirm that the pathology phenotypes of the *qsox1* mutant result from the T-DNA insertion into *QSOX1*, we constructed transgenic lines in the *qsox1* background that overexpress either QSOX1-HA or QSOX1-M3-HA (Supplemental Figure2C and 2D). Lines with elevated levels of *QSOX1-HA* or *QSOX1-M3-HA* transcripts, relative to native *QSOX1* transcript, were identified by RT–PCR and confirmed by anti-HA immunoblotting to accumulate QSOX1-HA and QSOX1-M3-HA proteins to levels correlating with transcript accumulation. QSOX1-HA ($QSOX1^{OE}$) lines no. 1 and no. 4 and QSOX1-M3-HA ($QSOX1\text{-}M3^{OE}$) lines no. 2 and no. 3 were selected for further analysis. When not specified, $QSOX1^{OE}$ and $QSOX1\text{-}M3^{OE}$ hereafter refer to line no. 4 and line no. 3, respectively.

The disease symptoms and growth caused by *Pst* DC3000 were tested in $QSOX1^{OE}$ and $QSOX1\text{-}M3^{OE}$ (Figure 3A and 3B). $QSOX1^{OE}$ plants complemented the phenotype of the *qsox1* mutant and also showed more severe disease symptoms and permitted more bacterial growth. On the contrary, the disease symptoms and bacterial growth observed in the $QSOX1\text{-}M3^{OE}$ plants were indistinguishable from the *qsox1* mutant. These data support the conclusions that QSOX1, dependent on its redox activity, is a negative regulator of *Arabidopsis* basal defense against *Pst* DC3000.

Expression of *Pathogenesis Related1* (*PR1*), deposition of callose in plant cell walls, and a rapid ROS burst are hallmarks of plant basal defense responses (Loon and Strien, 1999; Torres and Dangl, 2005; Jin and Mackey, 2017). *PR1* expression depends

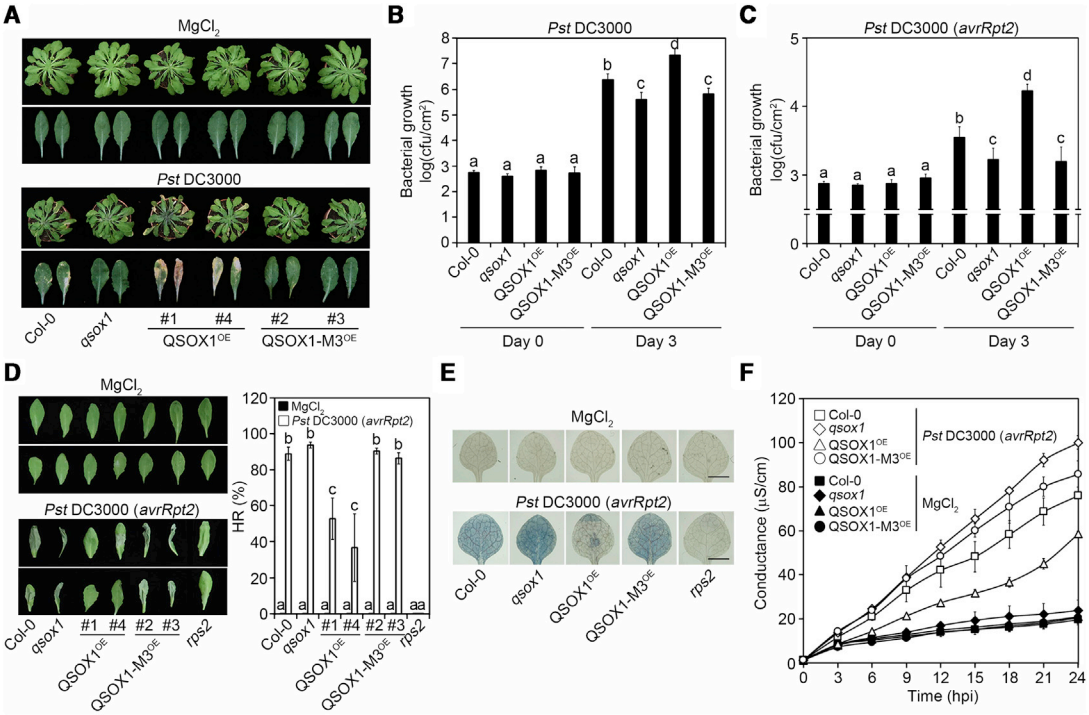

Figure 3. QSOX1 negatively regulates basal and HR defense against *P. syringae*.

(A) Disease symptoms of whole plants and leaves 3 days after spray inoculation with 10^6 cfu/ml of *Pst* DC3000.

(B) Bacterial growth analysis of *Pst* DC3000 after infiltration with 10^4 cfu/ml into the leaves of 4- to 5-week-old plants of the indicated genotypes. Different letters above bars represent significant differences ($P \leq 0.05$) according to a Tukey test.

(C) Bacterial growth analysis of *Pst* DC3000 (*avrRpt2*) after infiltration with 10^4 cfu/ml into the leaves of 4- to 5-week-old plants of the indicated genotypes.

(D–F) Measurement of the HR induced by AvrRpt2. Leaves of 4-week-old plants of the indicated genotypes were infiltrated with 10 mM $MgCl_2$ or 5×10^7 cfu/ml of *Pst* DC3000 (*avrRpt2*) and representative leaves were photographed after 12 h. The percentage of leaves showing macroscopic HR are presented at the right of the photographs **(D)**. Two-week-old plants of the indicated genotypes were vacuum infiltrated with 10 mM $MgCl_2$ or 10^8 cfu/ml of *Pst* DC3000 (*avrRpt2*) and individual leaves were stained with Evans blue after 18 h. Scale bars correspond to 2.0 mm **(E)**. Similarly, infiltrated leaf discs were sampled at the indicated time points for measuring ion leakage **(F)** (solid symbols infiltrated with 10 mM $MgCl_2$ and hollow symbols with the bacteria).

(B–D) Different letters above the bars represent significant differences ($P \leq 0.05$) according to a Tukey test. See also Supplemental Figures 2 and 3 and Supplemental Table 1.

largely on SA-induced, redox-mediated conversion of NPR1 from cytoplasmically localized multimers to monomers that move into the nucleus and function as transcriptional co-factors (Despres et al., 2003; Mou et al., 2003). Thus, we examined the role of *QSOX1* in *PR1* expression at 6, 12, and 18 h after infiltration of wild-type, *qsox1*, QSOX1^{OE}, and QSOX1-M3^{OE} plants with *Pst* DC3000 (Figure S3A). As expected, the abundance of *PR1* transcripts increased after infection of wild-type Col-0 (Wildermuth et al., 2001; Qi et al., 2018). Notably, expression of *PR1* was more strongly induced in the *qsox1* and QSOX1-M3^{OE} plants and less strongly induced in QSOX1^{OE} plants. Thus, consistent with its function as a negative regulator of disease resistance, QSOX1 negatively regulates *Pst* DC3000-induced *PR1* expression. Callose deposition and a rapid burst of ROS are induced by microbe-associated molecular patterns, such as flg22. However, these pattern-triggered immune (PTI) responses are likely unrelated to the role of QSOX1 in basal defense since they did not differ between Col-0, *qsox1*, QSOX1^{OE}, and QSOX1-M3^{OE} plants (Supplemental Figure 3B and 3C).

QSOX1 is a negative regulator of ETI in *Arabidopsis*

The known role of reactive oxygen to the HR and defense responses during ETI (Tsuda and Katagiri, 2010) prompted us to investigate the contribution of *QSOX1* to ETI elicited by strains of *Pst* DC3000 expressing type III effectors recognized by *Arabidopsis* NLRs. The strains tested were *Pst* DC3000 (*avrRpt2*), *Pst* DC3000 (*avrRpm1*), and *Pst* DC3000 (*avrRps4*), which elicit ETI in *Arabidopsis* dependent on the RPS2 and RPM1 CNLs and the RPS4/RRS1 dual pair of TNLs, respectively (Bent et al., 1994; Mindrinos et al., 1994; Grant et al., 1995; Zhang et al., 2004; Narusaka et al., 2009; Huh et al., 2017; Halane et al., 2018). We first checked the effect of QSOX1 on RPS2-induced *PR1* expression. As observed for *Pst* DC3000, the induction *PR1* transcript accumulation by *Pst* DC3000 (*avrRpt2*) was greater in *qsox1* and QSOX1-M3^{OE} and lesser in QSOX1^{OE} plants, relative to Col-0 (Supplemental Figure 3D). Thus, QSOX1 also negatively regulates *PR1* induction during ETI.

Next we investigated the effect of QSOX1 on bacterial growth restriction during ETI. The three NLR-activating bacterial strains were infiltrated at a low density into the leaves of Col-0, *qsox1*, QSOX1^{OE}, and QSOX1-M3^{OE} plants. As expected, ETI reduced the proliferation of each strain, relative to *Pst* DC3000, at 3 days after infiltration in Col-0 (compare Figure 3B with 3C, and Supplemental Figure 3E and 3F). Notably, relative to Col-0,

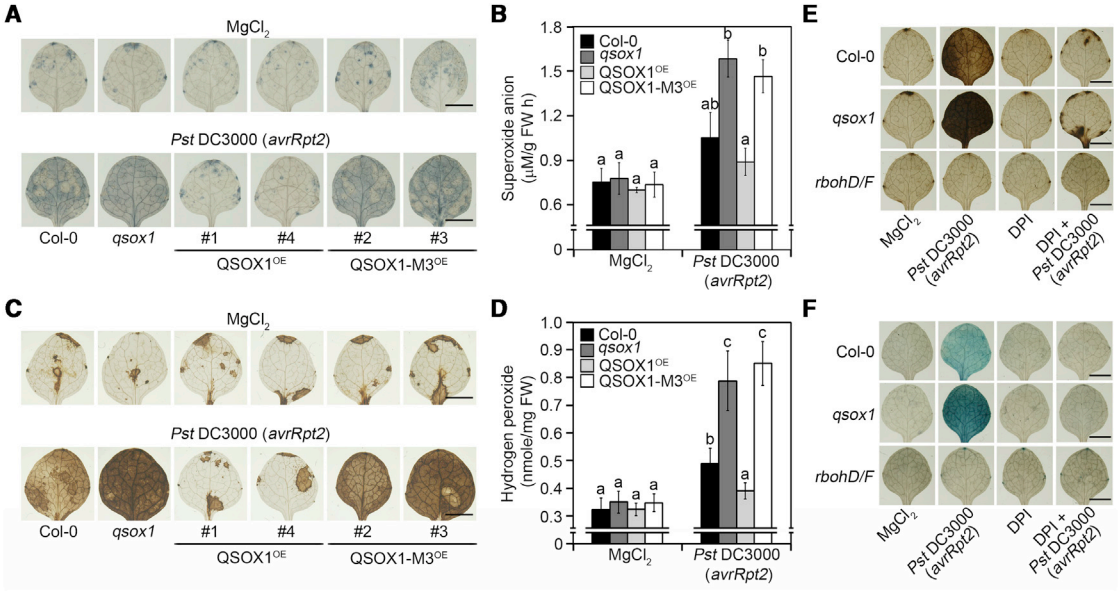

Figure 4. QSOX1 negatively regulates pathogen-induced, RBOH-dependent ROS accumulation.

(A and B) Detection of superoxide anion by NBT staining. Two-week-old *Arabidopsis* of the indicated genotypes were vacuum infiltrated with 10 mM $MgCl_2$ or *Pst* DC3000 (*avrRpt2*). After 18 h, the whole plants were immersed in a solution containing 1 mM NBT for 12 h and then photographed **(A)** or leaf discs were immersed in a solution containing 0.01% NBT and the oxidized NBT was quantified spectrophotometrically at A580 **(B)**.

(C and D) Detection of hydrogen peroxide (H_2O_2) by DAB staining with plants infiltrated as in **(A)** and incubated for 18 h. Brown staining in photographed leaves indicates polymerization of DAB in the presence of H_2O_2 **(C)**. Fluorescence signal was measured using 10-acetyl-3,7-dihydroxyphenoxazine to detect H_2O_2 concentration **(D)**.

(E) Detection of H_2O_2 by DAB staining in leaves of Col-0, *qsox1*, and *rbohD/F* plants 18 h after infiltration with buffer (10 mM $MgCl_2$) or *Pst* DC3000 (*avrRpt2*) in the presence or absence of 20 μM DPI.

(F) Cell death by Evans blue staining in the leaves of Col-0, *qsox1*, and *rbohD/F* plants 18 h after infiltration with buffer (10 mM $MgCl_2$) or *Pst* DC3000 (*avrRpt2*) in the presence or absence of 20 μM DPI. Scale bars correspond to 2.0 mm. **(B and D)** Different letters above bars represent significant differences ($P \leq 0.05$) according to a Tukey test.

See also Supplemental Figures 2 and 4 and Supplemental Table 1.

each ETI-eliciting strain proliferated less in *qsox1* and QSOX1-M3^{OE} plants and more in QSOX1^{OE} plants (Figure 3C and Supplemental Figure 3E and 3F). These results, which parallel the observed effect of QSOX1 on the growth of virulent *Pst* DC3000, indicate that QSOX1 also negatively regulates bacterial growth restriction during CNL- or TNL-dependent ETI.

In Col-0, ETI elicited by the CNLs, RPS2, and RPM1 is accompanied with an HR. The contribution of QSOX1 to HR was determined by challenging Col-0, *qsox1*, QSOX1^{OE}, and QSOX1-M3^{OE} plants with *Pst* DC3000 (*avrRpt2*) or *Pst* DC3000 (*avrRpm1*). Bacteria were infiltrated at a high density so that the cell death response, which is limited to isolated, individual cells that encounter bacteria during a natural or low-titer infection, instead becomes confluent and macroscopic. The macroscopic HR against *Pst* DC3000 (*avrRpt2*), which was absent as expected in *rps2* mutant plants, was observed with a similar, high frequency in Col-0, *qsox1*, and QSOX1-M3^{OE} plants and less frequently in QSOX1^{OE} plants (Figure 3D). Cell death associated with the HR can be visualized by Evans blue staining and measured quantitatively as an increase in conductivity caused by electrolyte leakage from dead cells into a bath solution. These assays reveal that *Pst* DC3000 (*avrRpt2*) or *Pst* DC3000 (*avrRpm1*) induces a similar level of cell death in Col-0, *qsox1*, and QSOX1-M3^{OE} plants, but a reduced level in QSOX1^{OE} plants (Figure 3E, 3F and Supplemental Figure 3G and 3H). Collectively, these results indicate that QSOX1 negatively regulates multiple outputs of ETI, including HR-associated cell death, induction of *PR1* transcription, and ultimately restriction of bacterial growth.

QSOX1 regulates RBOH-mediated ROS accumulation during ETI in *Arabidopsis*

The ability of QSOX1 to negatively regulate ETI, including HR, dependent on the redox-active cysteines in its Trx and ERV/ALR domains, led us to hypothesize that it is a redox sensor regulating the accumulation or processing of ROS during ETI. To explore this possibility, we examined the levels of superoxide anion (O_2^-) and hydrogen peroxide (H_2O_2) after infiltration of *Pst* DC3000 (*avrRpt2*) into young Col-0, *qsox1*, QSOX1^{OE}, and QSOX1-M3^{OE} plants. Qualitative (Figure 4A) and quantitative (Figure 4B) detection, by staining with nitroblue tetrazolium (NBT), revealed that QSOX1 negatively regulates accumulation of $O_2^{\cdot-}$. Relative to Col-0, more $O_2^{\cdot-}$ accumulated in *qsox1* and QSOX1-M3^{OE} plants. $O_2^{\cdot-}$ also accumulated to lower levels in QSOX1^{OE} plants; however, the difference was not significant between Col-0 and QSOX1^{OE}, possibly because the signal was close to the high background produced by the vasculature in the assay. Results for H_2O_2, based on DAB staining, paralleled those for $O_2^{\cdot-}$; relative to Col-0, *qsox1*, and QSOX1-M3^{OE} plants accumulated more and QSOX1^{OE} accumulated less H_2O_2 (Figure 4C and 4D). The results in Figure 4A–4D are measured

at 18 h after bacterial infiltration. Notably, the status of QSOX1 does not influence the burst of ROS observed during the first hour after bacterial challenge (Supplemental Figure 4A). To assess the generality of these findings, leaves of the same plants also were infiltrated with *Pst* DC3000 (*avrRpm1*) or *Pst* DC3000 (*avrRps4*) and stained with DAB. Similar to the results observed after RPS2 activation (Figure 4C), H_2O_2 produced during activation of RPM1 or RPS4/RRS1 were enhanced, relative to Col-0, in *qsox1* and QSOX1-M3^{OE} plants and reduced in QSOX1^{OE} plants (Supplemental Figure 4B and 4C). Collectively, these results demonstrate that QSOX1 negatively regulates reactive oxygen production during the later stage of ETI in *Arabidopsis*.

Because RBOHs are a primary source of ROS during plant immune responses, including the HR (Marino et al., 2012; Kadota et al., 2015), we surmised these enzymes to be a likely source of QSOX1-regulated ROS during ETI. To test this hypothesis, we examined the effect of the flavoprotein inhibitor, diphenyleneiodonium (DPI), on ROS generation and HR cell death in Col-0, *qsox1*, and *rbohD/F* plants after infiltration with *Pst* DC3000 (*avrRpt2*) (Figure 4E and 4F). In Col-0 plants, DPI inhibited the accumulation of H_2O_2 and the induction of cell death after activation of RPS2. As already demonstrated, HR cell death and the accumulation of H_2O_2 were increased in *qsox1* relative to Col-0. Notably, DPI dramatically reduced these exaggerated responses in *qsox1*. The accumulation of H_2O_2 and HR were absent in the *rbohD/F* mutant plants, indicating that the *qsox1* mutation and DPI were influencing RBOHD/F-dependent responses (Figure 4E and 4F). To once again examine the generality of these findings, similar experiments were conducted after infiltration of *Pst* DC3000 (*avrRpm1*) or *Pst* DC3000 (*avrRps4*) into Col-0 or *qsox1* (Supplemental Figure 4D–4F). Again, the accumulation of H_2O_2 and HR-associated cell death observed in Col-0 and these exaggerated responses in *qsox1* were reduced markedly in the presence of DPI to similar, low levels. An alternative, and non-exclusive explanation for the effect of QSOX1 on ROS accumulation is via effects on ROS scavenging enzymes. Measurement of catalase and ascorbate peroxidase activities revealed that the basal activity of these enzymes was unaffected by the status of QSOX1 (Supplemental Figure 4G and 4H). Interestingly, 24 h after infiltration with *Pst* DC3000 (*avrRpt2*) these scavenging activities, relative to Col-0 plants, were equal or higher in *qsox1* or QSOX1-M3^{OE} plants and equal or lower in QSOX1^{OE} plants (Supplemental Figure 4G and 4H). Thus, the activity of these ROS scavengers is unlikely to account for the influence of QSOX1 on ROS accumulation. On the contrary, the influence of QSOX1 on ROS accumulation may drive compensatory changes in ROS scavenger activity. Collectively, these results indicate that (1) QSOX1 negatively regulates RBOHD/F-dependent ROS production during ETI from activation of multiple NLRs and (2) elevated ROS produced by RBOHD/F contributes to the exaggerated, NLR-dependent cell death observed in the *qsox1* mutant.

QSOX1 regulates RBOH-mediated ROS production indirectly by interacting with and oxidatively inactivating GSNOR

The primary source of ROS during *Arabidopsis* defense, including ETI, is the NADPH oxidase AtRBOHD (hereafter RBOHD [Torres et al., 2002]). Thus, our first hypothesis was that QSOX1 regulates either constitutive or ETI-induced expression of *RbohD*. To test this possibility, we measured *RbohD* transcript levels in Col-0, *qsox1*, QSOX1^{OE}, and QSOX1-M3^{OE} plants before and after challenge with *Pst* DC3000 (*avrRpt2*), *Pst* DC3000 (*avrRpm1*), or *Pst* DC3000 (*avrRps4*). The baseline level of *RbohD* transcript, as well as its modest induction from 12 to 48 h after infiltration with each of the ETI-eliciting bacteria, was unaffected by mutation or overexpression of *QSOX1* (Supplemental Figure 4I). These data refute the hypothesis that QSOX1 regulates ROS levels by affecting expression of *RbohD*. A second hypothesis was that QSOX1 interacts with RBOHD. However, neither co-immunoprecipitation nor bimolecular fluorescence complementation (BiFC) following transient expression in *Nicotiana benthamiana* detected such an interaction (Figure 5A and 5C, respectively). These findings led us to consider that QSOX1 regulates the activity of RBOHD indirectly.

A candidate for indirect regulation of RBOHD is the S-nitrosoglutathione reductase, AtGSNOR (hereafter GSNOR). During ETI, elevated levels of reactive nitrogen species (RNS), including GSNO, inactivate RBOHD through S-nitroylation of a conserved, regulatory cysteine and resulting ejection of FAD from the enzyme (Yun et al., 2011). Given that GSNOR is primarily responsible for GSNO catabolism in plants and thus provides a potential regulatory link to RBOHD, we hypothesized that QSOX1 interacts with GSNOR. Indeed, interaction of QSOX1 and GSNOR was detected by both co-immunoprecipitation (co-IP) and BiFC following expression in *N. benthamiana* (Figure 5B and 5C). The BiFC signal from interaction of QSOX1-YN with YC-GSNOR overlaps with that from FM4-64, which labels the plasma membrane (Figure 5D). Furthermore, the M1-, M2-, and M3-cysteine mutant derivatives of QSOX1 maintained the ability to co-IP with GSNOR (Figure 5E). Thus, independent of its oxidoreductase activity, QSOX1 interacts with GSNOR at the cell periphery *in planta*.

Plant GSNORs contain nine positionally conserved cysteines that are not involved in zinc coordination, three of which are predicted to be surface exposed, raising the possibility that reversible thiol oxidation regulates GSNOR function (Xu et al., 2013). Indeed, non-reducing SDS–PAGE revealed that GSNOR exists in DTT-sensitive dimers and higher-molecular-weight oligomers (Figure 5F). Thus, we formed a two-part hypothesis that (1) the burst of ROS during a plant immune response induces oxidation of QSOX1 and (2) oxidized QSOX1 subsequently oxidizes its client protein, GSNOR. These hypotheses were tested *in vivo* by infiltrating QSOX1^{OE} or QSOX1-M3^{OE} plants with *Pst* DC3000 (*avrRpt2*) and then measuring the oxidation state of the QSOX1-HA or QSOX1-M3-HA and native GSNOR proteins. Samples immunoprecipitated with anti-HA or anti-GSNOR antibodies were split and proteins in the subsamples were either biotinylated on reduced thiols by treatment with biotin-HPDP or were biotinylated on oxidized thiols by sequentially blocking reduced thiols with N-ethylmaleimide (NEM), reducing S-nitrosylated cysteines with ascorbate or S-nitrosylated and dithiol cysteines with DTT, and then treating them with biotin-HPDP (Supplemental Figure 5). Subsequent protein blotting to detect biotin established relative levels of the oxidized and reduced proteins while immunoblotting of the initial extracts against HA or GSNOR demonstrated total levels of QSOX1 or GSNOR, respectively.

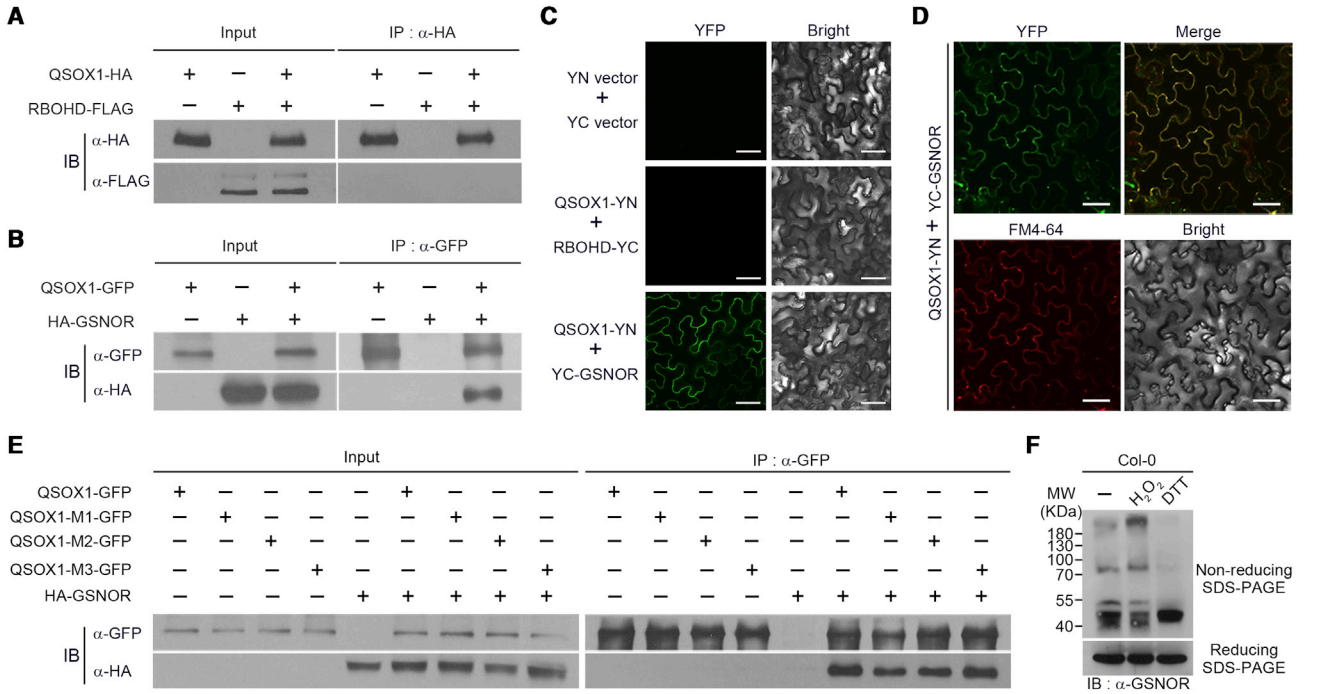

Figure 5. QSOX1 interacts with GSNOR *in planta,* but not with RBOHD.

(A) RBOH fails to co-immunoprecipitate with QSOX1 following agro-transient expression in *N. benthamiana* leaves. IP was performed using an anti-HA (QSOX1-HA) antibody followed by immunoblotting with anti-HA and anti-FLAG (RBOHD-FLAG) antibodies.

(B) Co-IP of QSOX1 and GSNOR expressed by agro-transient in *N. benthamiana* leaves. IP was performed with anti-GFP (QSOX1-GFP) antibody followed by immunoblotting with an anti-GFP and anti-HA (HA-GSNOR) antibodies.

(C and D) Bimolecular fluorescence complementation (BiFC) assay. Confocal images of *N. benthamiana* leaves following agro-transient expression of fusions of QSOX1 and GSNOR or RBOHD, with the N-terminal of YFP and the C-terminal of YFP (YN or YC), respectively **(C)**. BiFC detection of QSOX1–GSNOR interaction of which fluorescence was overlapped with that of FM4-64 used as a standard marker of plasma membrane **(D)**. Scale bars correspond to 50 μm.

(E) Co-IP of GSNOR with native form of QSOX1 or its mutant derivatives following agro-transient expression in *N. benthamiana* leaves as in **(B)**.

(F) Redox-dependent structural changes of GSNOR *in vivo*. Leaf extracts from 2-week-old wild-type plants were prepared and treated with 1 mM H_2O_2 or 1 mM DTT for 1 h. Protein structure of GSNOR was determined by western blotting using anti-GSNOR antibody following separation on non-reducing (top) and reducing (bottom) SDS–PAGE.

See also Supplemental Figure 4 and Supplemental Table 1.

QSOX1-HA existed primarily in a reduced state before *Pst* DC3000 (*avrRpt2*) infiltration, but a significant portion became oxidized by 12 h after infiltration and remained so for at least 48 h (Figure 6A). The low levels of biotinylated oxidized or reduced forms of QSOX1-M3-HA, which lack the six reactive cysteines found in its Trx and ERV/ALR domains, did not vary after bacterial infiltration (Figure 6B). Notably, the overall levels of QSOX1-HA and QSOX1-M3^{OE}-HA remained similar before and after infiltration with *Pst* DC3000 (*avrRpt2*) (Figure 6A and 6B, bottom blot). These data support the first part of our hypothesis that the reactive cysteines of QSOX1 becomes oxidized following challenge with *Pst* DC3000 (*avrRpt2*), presumably by sensing the elevated ROS that accumulates upon induction of ETI.

The data also support the second part of our hypothesis that oxidized QSOX1 subsequently oxidizes GSNOR. In QSOX1^{OE} plants, GSNOR is primarily reduced before infiltration and, after infiltration with *Pst* DC3000 (*avrRpt2*), becomes progressively more oxidized from 12 to 48 h (Figure 6C). Consistent with GSNOR being a client protein of oxidized QSOX1, the timing of GSNOR oxidation lags behind that of QSOX1-HA (compare Figure 6A and 6C). In QSOX1-M3^{OE} plants, which lack native QSOX1 and express only the redox inactive QSOX1-M3-HA derivative that still interacts with GSNOR or *qsox1* plants, the level of oxidized GSNOR does not increase after infiltration of *Pst* DC3000 (*avrRpt2*) (Figure 6D and 6E). The same pattern of GSNOR oxidation, dependent on wild-type QSOX1, was also observed in experiments using *Pst* DC3000 (*avrRpm1*) and *Pst* DC3000 (*avrRps4*) (Supplemental Figure 6A and S6B). Collectively these data indicate that QSOX1 senses the reactive oxygen burst during ETI by shifting its equilibrium from the reduced to the oxidized form and that oxidized QSOX1 then oxidizes its client protein, GSNOR.

Establishing that GSNOR is a client protein oxidized by QSOX1 led us to predict that QSOX1-dependent oxidation negatively regulates GSNOR enzymatic activity. GSNOR activity was measured before and 4, 8, 12, 24, and 48 h after infiltration with *Pst* DC3000 (*avrRpt2*) by quantifying the oxidative consumption of NADH dependent on the addition of the substrate, GSNO, to leaf extracts (Figure 6F). As expected, minimal enzymatic activity was detected in control plants lacking GSNOR (*gsnor1-3*). Before bacterial infiltration, GSNOR activity did not differ between Col-0, *qsox1*, QSOX1^{OE}, and QSOX1-M3^{OE} plants.

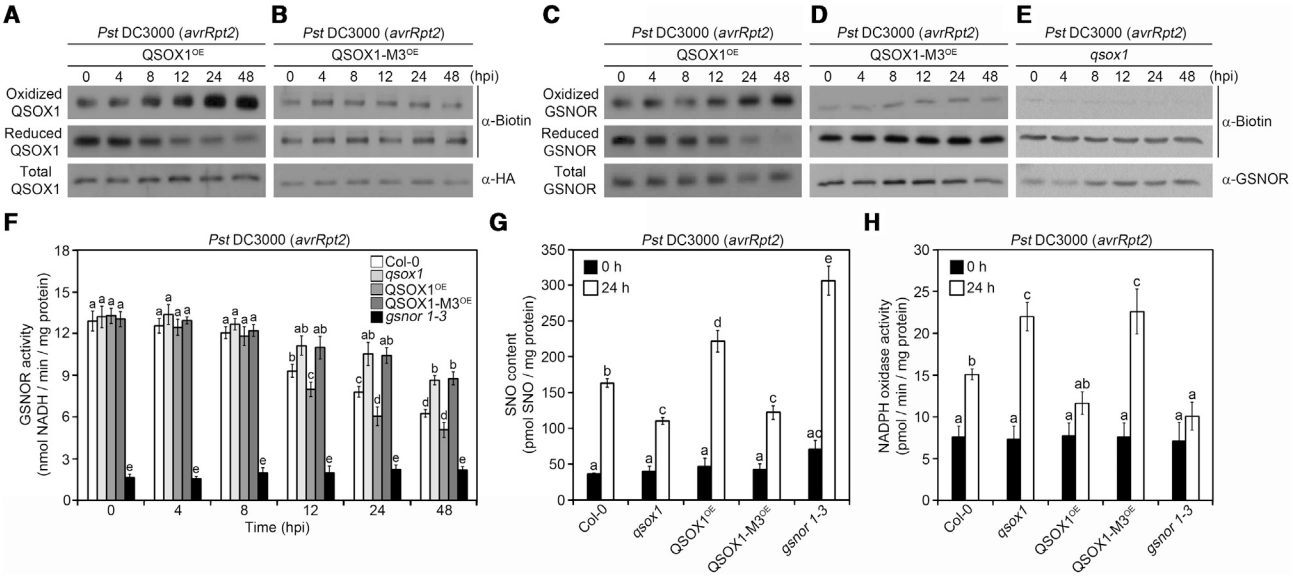

Figure 6. QSOX1 mediates pathogen-induced inhibition of GSNOR activity through a redox relay.

(A–E) Redox status of reactive Cys residues of QSOX1 and GSNOR *in vivo* before and after inoculation of *Pst* DC3000 (*avrRpt2*). Leaves of 2-week-old QSOX1^{OE} **(A and C)**, QSOX-M3^{OE} **(B and D)**, or *qsox1* **(E)** were infiltrated with 10^8 cfu/ml of *Pst* DC3000 (*avrRpt2*) and leaf extracts were prepared at the indicated hours post-inoculation (hpi). As outlined in Supplemental Figure 5, samples were immunoprecipitated with anti-HA (QSOX1) **(A and B)** or anti-GSNOR (GSNOR) antibodies **(C–E)** and the subsamples were processed to biotinylate oxidized or reduced cysteines and immunoblotted with anti-biotin antibodies. To determine total levels of QSOX1 and GSNOR, respectively, initial extracts were immunoblotted with either anti-HA **(A and B)** or anti-GSNOR **(C–E)** antibody.

(F) GSNOR activity in leaf extracts of the indicated plants was determined at the indicated times after infiltration with *Pst* DC3000 (*avrRpt2*) by measuring the GSNO-dependent oxidation of NADH.

(G and H) Total SNO levels **(G)** or NADPH oxidase activity **(H)** are shown for leaf extracts from 2-week-old plants of the indicated genotypes before (solid bars) or 24 h after (hollow bars) infiltration with 10^8 cfu/ml of *Pst* DC3000 (*avrRpt2*). Values were normalized against whole-plant lysate protein content. These experiments were repeated at least three times with similar results. Different letters above bars represent significant differences ($P \leq 0.05$) according to a Tukey test.

See also Supplemental Figures 2, 5, and 6 and Supplemental Table 1.

GSNOR activity of all four plant lines decreased between 12 and 48 h after infiltration of *Pst* DC3000 (*avrRpt2*), but the extent of the reduction differed significantly between the lines. Relative to Col-0, GSNOR activity remained higher in *qsox1* and QSOX1-M3^{OE} and was lower in QSOX1^{OE}. These data indicate that QSOX1-dependent oxidation of GSNOR correlates with a reduction of its enzymatic activity in leaf extracts tested *in vitro*.

We hypothesized that QSOX1-mediated, negative regulation of GSNOR activity also occurs *in planta* and tested the prediction by measuring levels of S-nitrosylated (SNO) protein (Figure 6G). Reduction of GSNO by GSNOR reduces the pool of GSNO available to nitrosylate proteins. Before infiltration with *Pst* DC3000 (*avrRpt2*), the SNO protein levels did not differ significantly between Col-0, *qsox1*, QSOX1^{OE}, QSOX1-M3^{OE}, and *gsnor1-3* plants. After infiltration, SNO protein levels increased significantly in all five plant lines, but, as observed for the *in vitro* activity of GSNOR, the extent of the increase differed significantly between the lines. Specifically, relative to Col-0, SNO protein levels were higher in QSOX1^{OE} and *gsnor1-3* and lower in *qsox1* and QSOX1-M3^{OE}. Thus, the extent of increase in SNO protein levels in each plant type inversely correlated with the *in vitro* activity of GSNOR measured in Figure 6F. The generality of these findings after infiltration with *Pst* DC3000 (*avrRpt2*) is apparent from the similar effects of QSOX1 status on SNO protein levels after infiltration with *Pst* DC3000 (*avrRpm1*) or *Pst* DC3000 (*avrRps4*) (Supplemental Figure 6C and 6D). Thus, the data collectively support the hypothesis that QSOX1-dependent oxidation inactivates GSNOR *in planta*.

Increased levels of GSNO resulting from the oxidative inactivation of GSNOR by QSOX1 likely influence SNO levels of many target proteins. To assess the potential role of S-nitrosylation on the GSNOR-RBOHD signaling module, we measured the level of S-nitrosylation of each protein following challenge with *Pst* DC3000 (*avrRpt2*). In QSOX1^{OE} plants, GSNOR was S-nitrosylated to low but progressively increasing levels and with similar timing relative to its oxidation to dithiols (Supplemental Figure 6E, compare with Figure 6C), hinting at potential feedback regulation of GSNOR by increasing levels of GSNO. More closely related to the central model presented in this work, levels of S-nitrosylated RBOHD at 24 h after bacterial challenge were, relative to Col-0, reduced in *qsox1* and QSOX1-M3^{OE} plants and elevated in QSOX1^{OE} and *gsnor1-3* plants (Supplemental Figure 6F). These results parallel those for NADPH oxidase activity (Figure 6H) and further point to QSOX1-mediated inactivation of GSNOR leading to S-nitrosylation-mediated inactivation of RBOHD.

DISCUSSION

In this study, we identify QSOX1 as a functional, redox-responsive oxidoreductase that, during plant immune responses,

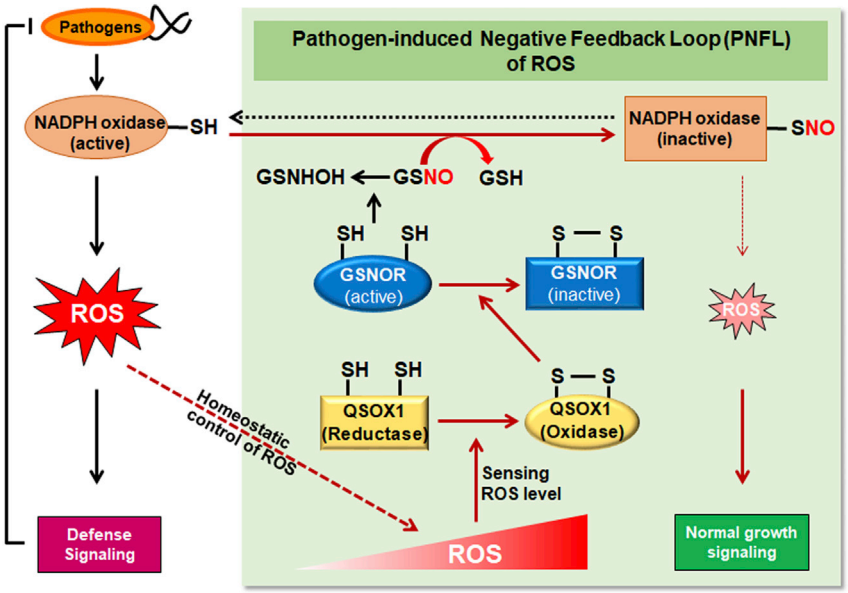

Figure 7. A working model deciphering how QSOX1 functions as a key regulator of plant immunity.

Plants generate an initial burst of ROS following a pathogenic attack. The extent of ROS production is regulated to limit harmful consequences to plant growth and metabolism, as well as to balance with levels of RNS to regulate defense outputs. Our results support the "pathogen-induced negative feedback loop" (PNFL) of ROS model, which suggests that the redox sensor QSOX1, following oxidative activation upon an initial immune-associated ROS burst, in turn oxidizes and inactivates its client protein GSNOR, which ultimately leads to increased levels of GSNO and S-nitrosylated protein content of the plant. One consequence is reduced activity of S-nitrosylated NADPH oxidase, which effectively limits the extent of ROS production. These signaling cascades can be followed by red lines with arrows.

senses initial and limits subsequent ROS accumulation. Taken together, our data support a model for the QSOX1-mediated, homeostatic control of ROS through a regulatory circuit designated as a "pathogen-induced negative feedback loop" (PNFL) (Figure 7). Central to the model is the oxidative activation of QSOX1 upon its sensing of an initial, immune-associated ROS burst. Activated QSOX1 in turn oxidizes and inactivates its client protein, GSNOR, which causes an increase in available GSNO and S-nitrosylated proteins, including RBOHD. These findings, along with previous work indicating that GSNOR activity limits S-nitrosylation-mediated inactivation of RBOHD, provide a mechanistic explanation for how QSOX1 reduces the magnitude of RBOH-dependent ROS production, limits the extent of HR-type cell death, and, ultimately, negatively regulates the restriction of bacterial growth during plant immune responses. The rapid burst of pathogen-induced ROS that is sufficient to activate plant defense signaling precedes SNO-mediated inhibition of RBOHD resulting from subsequent QSOX1-mediated oxidation of GSNOR. Similar to our model, abscisic acid (ABA)-induced stomatal closure was desensitized by the inactivation of RBOHD by S-nitrosylation in water-deficit conditions. During the process, ABA rapidly transduced its signaling through SnRK2.6 activation and S-nitrosylation of SnRK2.6 subsequently feedback inhibited the ABA signaling (Wang et al., 2015b; Balmant et al., 2016). Thus, our results provide a finely tuned molecular mechanism for the feedback inhibition of pathogen-mediated immune signaling in plants that is reminiscent of similar mechanisms in guard cells regulating stomates in plants (Wang et al., 2015a) and T cells regulating immune tolerance in mammals (Sakaguchi et al., 2008).

QSOX1 negatively regulates distinct branches of the plant immune system. These include basal defense against a virulent pathogen (*Pst* DC3000) and ETI against avirulent strains of *Pst* DC3000 expressing type III effectors that activate either CNL or TNL resistance proteins. The lack of effect of QSOX1 on PTI indicates that it alternatively influences basal defense. Given the involvement of ROS signaling in both basal defense and ETI, the QSOX1-GSNOR-RBOH-based PNFL for homeostatic control of ROS production likely contributes to the regulation of each. However, the veracity of the proposed PNFL model excludes neither redox-based regulation of QSOX1-client proteins other than GSNOR nor effects of GSNOR regulation other than influencing the activity of RBOHs. Indeed, distinctions between the phenotype of *qsox1* and *gsnor* or *rbohd* mutant plants (Torres et al., 2002; Torres and Dangl, 2005; Miller et al., 2009; Pogany et al., 2009; Malik et al., 2011; Kadota et al., 2015) indicate that QSOX1 likely regulates additional aspects of plant immunity.

Overlaid onto the biochemical modification of client protein(s) by QSOX1 is nuanced regulation of *QSOX1* expression in response to biotic stress. Induced accumulation of *QSOX1* transcripts, by pathogen exposure or mobile defense hormones, likely tunes QSOX1 activity at different times and in different cells or tissues. For example, regulated expression of *QSOX1* may influence the PNFL for ROS homeostasis during biotic stress. Relatively lower levels of QSOX1 in naive cells, such as at a primary site of infection, may permit sustained activity from RBOHs that contributes to a robust initial defense response, including local HR that can effectively control the spread of avirulent pathogens. One consequence of this initial response is the production of mobile defense hormones, including SA and JA, which can induce the expression of *QSOX1* and more generally alter the immune competence of uninfected cells both nearby to a primary site of infection as well as systemically. Along with heightened resistance, increased QSOX1 activity in these nearby cells or distal tissues likely limits oxidative stress by shortening the duration and/or reducing the intensity of ROS production. Thus, QSOX1-mediated ROS homeostasis, as well as other possible QSOX1-regulated immune functions, may be different between primary and spreading or distal sites of infection.

Crosstalk between ROS and RNS has been widely observed to influence plant immune responses (Frederickson Matika and Loake, 2014). The production, processing, and output activity of these redox-active molecules are co-regulated and interconnected.

For example, cytosolic Ca^{2+} contributes to the production of both ROS and nitric oxide (NO). Ca^{2+}-dependent protein kinases contribute to the rapid activation of RBOHs during plant defense (Oda et al., 2010; Dubiella et al., 2013). The source of defense-induced NO production is still ambiguous, but likely involves both an oxidative, nitric oxide synthase-like pathway and an $H_2O_2^-$ and MPK6-regulated, nitrate reductase-like pathway, each of which require Ca^{2+} (Vandelle et al., 2016). NO pleiotropically regulates numerous signaling pathways relevant to plant defense, including ROS signaling. S-Nitrosylation of glutathione produces GSNO which, when not reduced by GSNOR, serves as an RNS reservoir and active signaling intermediate. GSNO inhibits both the production, by glycolate oxidase, and processing, by catalase, of H_2O_2 in the peroxisome (Ortega-Galisteo et al., 2012; Corpas and Barroso, 2014; Corpas et al., 2019). In addition, NO can differentially regulate ascorbate peroxidase through S-nitrosylation and tyrosine nitration to influence the ROS scavenging glutathione-ascorbate cycle (de Pinto et al., 2013; Begara-Morales et al., 2014; Yang et al., 2015). GSNO regulates the activity of RBOHs, the direct product of which is apoplastic $O_2^{\cdot-}$, which is rapidly converted to H_2O_2 by apoplastic and cytosolic superoxide dismutases (SODs) (Yun et al., 2011; Wang et al., 2016; Lightfoot et al., 2017). Alternatively, $O_2^{\cdot-}$ can interact efficiently with NO to form the potent nitrating and oxidizing molecule peroxynitrite ($ONOO^-$). Rather than directly promoting cell death, as in animal cells, $ONOO^-$, which accumulates during the HR in plants potentiates defense through alternative signaling output(s). $ONOO^-$ induces tyrosine nitrosylation, which inactivates the $ONOO^-$ detoxifying enzyme peroxiredoxin II E and, *in vitro*, inhibits the activity of multiple SODs. Thus, $ONOO^-$ may control HR through regulating the balance in levels of NO, $O_2^{\cdot-}$, and H_2O_2 (Delledonne et al., 2001; Romero-Puertas et al., 2007). QSOX1 adds a novel player to the defense-associated ROS/RNS-signaling network as an oxidatively activated sensor that, among likely numerous additional outputs, promotes accumulation of GSNO through inactivating GSNOR and, in turn, limits RBOH-mediated ROS production. By thus regulating the balance between ROS and RNS levels, QSOX1 likely influences various immune regulatory functions. One obvious candidate is the complex regulation of NPR1 signaling by SA, ROS, and RNS levels (Mou et al., 2003; Tada et al., 2008; Lindermayr et al., 2010; Kovacs et al., 2015; Ding et al., 2018). However, given that HR mediated by numerous R proteins, including RPM1, RPS2, and RPS4/RRS1, is largely or entirely independent of NPR1 signaling, additional mechanisms regulated by QSOX1 and possibly influenced by the balance of ROS and RNS likely contribute to the negative regulation of HR.

Our findings firmly establish a role of QSOX1 in plant immune responses. The extent of QSOX-mediated regulation in other stress and developmental contexts remains largely unknown. RBOH-mediated ROS production is a signature of various abiotic stresses, raising the immediate possibility that QSOX1 or QSOX2 influence ROS and RNS homeostasis via a mechanism directly analogous to the proposed PNFL (Balmant et al., 2016; Zhou et al., 2016). A previous study demonstrated that *Arabidopsis* plants overexpressing QSOX1 (therein referred to as Par1, for polyamine resistant1) are better able to tolerate exposure to polyamines (Alejandro et al., 2007). This raises the interesting possibility that the presence of QSOX1 counteracts an imbalance of ROS and RNS homeostasis that occurs during production of NO via oxidation of polyamines. More generally, ROS and RNS signaling has been implicated in various developmental processes, including germination, root growth, flower development, and flowering time, as well as interaction of roots with microorganisms in the rhizosphere (Pauly et al., 2006; El-Maarouf-Bouteau and Bailly, 2008; Airaki et al., 2015; Turkan, 2018). Whether QSOX1 and/or QSOX2 sense and signal in response to shifts in cellular redox status resulted from ROS generation at different sites, from cellular to tissue levels, during these various stress and developmental pathways awaits further investigations.

METHODS

Plant materials and growth conditions

Arabidopsis thaliana plants were all in the ecotype Columbia (Col-0). Transgenic lines of *Arabidopsis* overexpressing QSOX1-HA (line no. 4 = $QSOX1^{OE}$) and the Cys residues mutant QSOX1-M3-HA (line no. 3 = $QSOX1\text{-}M3^{OE}$) were generated in the *qsox1* mutant background (T-DNA insertion knockout, SALK_072829) using pGWB14 vector. To induce synchronous germination, seeds were vernalized at 4°C for 3 days before growth. Plants were grown under light at 100–120 μmol m^{-2} s^{-1} photosynthetic flux at 22°C, either in soil with 70% humidity and 8 h of light per day or in plates of $^1/_2$ MS medium, 2% sucrose and 0.25% phyta-gel (pH 5.8) with 16 h of light per day. The *rps2-101C* (Kunkel et al., 1993), *gsnor1-3* (Feechan et al., 2005) mutants were reported previously.

Bacterial pathogen inoculations

Bacterial strains used in this study were *P. syringae* pv. tomato DC3000, *Pst* DC3000 (*avrRpt2*), *Pst* DC3000 (*avrRpm1*), and *Pst* DC3000 (*avrRps4*). All strains were grown at 30°C on King's B medium containing the appropriate antibiotics for selection. Vacuum and spray were used to inoculate *Arabidopsis* plants. For vacuum inoculation, the bacteria were scraped off from a fresh plate, resuspended in 10 mM $MgCl_2$ containing 0.005% Silwet L-77 (Lehle Seeds, Round Rock, TX, USA) to 10^8 cfu/ml, and introduced by vacuum infiltration into submerged leaves of plants previously washed for 1 min in sterile distilled water. For spray inoculation, plants were sprayed with a bacterial suspension containing 10^6 cfu/ml bacteria with 0.005% Silwet L-77.

Purification of recombinant QSOX1 and its derivatives

E. coli BL21 ([DE3] pLysS) was transformed with pIH1119 encoding wild-type QSOX1 or derivatives with active site Cys residues replaced with Ser. The bacterial cells were cultured at 30°C in modified terrific broth (MTB) medium supplemented with ampicillin (50 μg/ml). When the optical density of the culture at 600 nm reached 0.5 to 0.6, isopropyl-β-D-thiogalacto-pyranoside (IPTG) was added to the culture at a final concentration of 0.2 mM and the cells were incubated for a further 4 h at 30°C. The cells were harvested by centrifugation at 9000 *g* for 6 min and the pellet was re-suspended in phosphate-buffered saline (PBS) buffer (containing 140 mM NaCl, 2.7 mM KCl, 10 mM Na_2HPO_4, and 1.8 mM KH_2PO_4 [pH 8.0]) with 1 mM PMSF and stored at −70°C until use. After the cells were disrupted by sonication, the MBP-fused QSOX1 proteins were purified with Amylose resin (New England Biolabs, Ipswich, MA, USA) and the QSOX1 proteins were separated from maltose binding protein (MBP) tag by thrombin cleavage (Roche, Basel, Switzerland).

Gene expression analysis of *QSOX1* and *RBOH*

To test the effect of biotic and abiotic stresses on *QSOX1* and *RBOH* gene expression, *Arabidopsis* plants (Col-0) grown in MS medium were exposed to various stresses. Plants were vacuum infiltrated with 10^8 cfu/ml *P. syringae* pv. *tomato* DC3000 and *P. syringae* pv. *tomato* DC3000 (*avrRpt2*), 2 mM SA, 100 μM MeJA, or 5 μM methyl viologen (MV). Also, plants were incubated at 4°C for "Cold" or at 37°C for "Heat" treatments. Plant tissues were sampled at the indicated time points, frozen

immediately in liquid nitrogen, and RNA was extracted using a NucleoSpin RNA Plant Kit (Macherey-Nagel, Düren, Germany). Two micrograms of total RNAs were reverse-transcribed using SuperScript II Reverse Transcriptase (Invitrogen, Carlsbad, CA, USA) and 1 μl oligo dT (Invitrogen, Carlsbad, CA, USA). One microliter of the resultant reaction mixture was used as a template for RT–PCR with the following reaction conditions; 5 min incubation at 95°C, followed by 25 cycles of 30 s at 95°C, 1 min at 51°C–58°C, 1 min at 72°C, and then 72°C for another 10 min for a final extension. *Tubulin* or *actin* was used as a control for cDNA preparation. Quantitative real-time PCR was performed with the StepOnePlus Real-Time PCR System (Applied Biosystems, Foster City, CA, USA) using a Power SYBR Green Master Mix (Applied Biosystems, Foster City, CA, USA) according to the manufacturer's protocol. PCR cycling conditions were as follows: 95°C for 10 min (1×), 95°C for 15 s/60°C for 1 min (40×), followed by a melting curve step to confirm the specificity of the amplified products. Amplification curves and gene expression were normalized to the housekeeping gene 18S, used as an internal standard.

Assay of oxidase and reductase activities of QSOX1

Reduced ribonuclease A (RNase A) prepared as described (Tu et al., 2000) was used to assess QSOX1 oxidase activity in the reaction buffer containing 100 mM Tris acetate (pH 8.0), 50 mM NaCl, and 1 mM EDTA. At the indicated reaction times, free thiols were blocked by the addition of SDS loading buffer and 10 mM AMS (4-acetamido-4′-maleimidylstilbene-2,2′-disulfonic acid) (Invitrogen, Carlsbad, CA, USA). The oxidized and reduced forms of RNase A were separated by non-reducing SDS–PAGE gel and visualized by staining with Coomassie brilliant blue. Disulfide reductase activity of QSOX1 was assayed with the substrate, DTNB (Sigma-Aldrich, St. Louis, MO, USA) at 25°C. QSOX1 proteins were added to the reaction mixture of 50 mM HEPES (pH 8.0) buffer containing 3 mM EDTA, 5 mM DTNB, 150 μM NADPH, and 0.1 μM AtNTRA, and the rate of DTNB reduction to produce 2TNB was measured using a spectrophotometer at A412.

NBT, DAB, and Evans blue staining

Two-week-old *Arabidopsis* seedlings were vacuum infiltrated with bacteria and incubated for 18 h. To detect the quantity of superoxide anion, the whole plants were immersed in a solution containing 1 mM NBT (Sigma-Aldrich, St. Louis, MO, USA) plus 10 mM sodium azide in 50 mM sodium phosphate buffer (pH 7.4) for 12 h, washed three times with distilled water, and de-stained with 90% ethanol. To detect hydrogen peroxide, detached leaves were detached and incubated in 1 mg/ml DAB (Sigma-Aldrich, St. Louis, MO, USA) solution (pH 6.0) for 12 h. To develop the reddish-brown coloration of the DAB polymer, stained leaves were placed in boiling (65°C) 90% ethanol for 30 min. To detect cell death by Evans blue staining, detached leaves were vacuum infiltrated with 0.1% (w/v) Evans blue solution for 20 min and placed in Evans blue solution (made up to 0.1% [w/v]) for 12 h before three washes with distilled water and de-staining with 90% ethanol. NBT-, DAB-, and Evans blue-stained leaves were visualized using a microscope (Olympus, SZX12). Plant growth conditions and bacterial treatment method were the same for NBT, DAB, Evans blue staining experiments.

Aniline blue staining

Four-week-old leaves of the indicated genotypes were hand infiltrated with water control or 1 μM flg22 using a 1 ml needleless syringe. After 24 h, leaves were fixed and cleared in a solution of 96% ethanol overnight, incubated for 30 min in 70 mM sodium phosphate buffer (pH 9), stained with 0.005% aniline blue solution for 60 min in the same buffer, followed by the addition of 0.1% calcofluor white. Observations were performed using a microscope (Olympus, AX70).

Quantitative assay of the superoxide anion and H_2O_2

Two-week-old *Arabidopsis* seedlings were vacuum infiltrated with bacteria and incubated for 18 h. For detection of the superoxide anion, three 5 mm diameter leaf discs were immersed in 3 ml of 0.01 M potassium phosphate buffer (pH 7.8) containing 0.01% (w/v) NBT and 10 mM sodium azide for 12 h in the dark. Leaf discs were removed from the reaction mixture and the remaining solution was boiled at 85°C for 15 min and cooled on ice. The oxidized NBT was then measured at A_{580}. For hydrogen peroxide detection, 200 mg of leaf tissue was ground with liquid nitrogen and resuspended in 500 μl potassium phosphate buffer (20 mM K_2HPO_4 [pH 6.5]). The extracts were centrifuged at 13 000 *g* for 15 min at 4°C and the supernatants were used for hydrogen peroxide assay. The concentration of hydrogen peroxide was measured using an Amplex Red hydrogen peroxide/peroxidase assay kit (Invitrogen, Carlsbad, CA, USA) and the fluorescence was detected using a microplate spectrofluorometer.

ROS production assay

Three leaf discs from 4-week-old plants (Col-0, *qsox1*, QSOX1^{OE}, and QSOX1-M3^{OE}) were collected and floated on sterile water overnight in 96-well plates. The water was removed and replaced with 100 μl of solution containing 10^8 cfu/ml of *Pst* DC3000 (*avrRpt2*), 5 mM luciferin (Biosynth International, Naperville, IL, USA), and 20 μg/ml horseradish peroxidase (Sigma-Aldrich, St. Louis, MO, USA). Luminescence was quantified by means of photon counts from each well using a CCD camera (Berthold, NightSHADE LB 985).

Assays for the measurement of antioxidant protein activity

Two-week-old *Arabidopsis* seedlings grown in $^1/_2$ MS media were vacuum infiltrated with bacteria and incubated for 24 h. The plants were ground to a fine powder in a pestle with liquid nitrogen. Catalase activity was analyzed with a Catalase Activity Assay Kit (Abcam, Cambridge, MA, USA) according to the manufacturer's instructions. The fluorescence of the samples was assessed using a spectrofluorometer at E_x/E_m = 535/587 nm. Ascorbate peroxidase activity was determined using an Ascorbate Peroxidase (APX) Activity Assay Kit (Elabscience, Beijing, China) according to the manufacturer's instructions. The absorbance of the samples was assessed using a spectrophotometer at A290.

Co-immunoprecipitation assay and BiFC

DNA constructs of GFP-tagged QSOX1 (QSOX1-GFP) and HA-tagged GSNOR (HA-GSNOR) were co-expressed by agro-transient infiltration in 3- to 4-week-old *N. benthamiana* leaves. The leaf tissue harvested after 3 days was ground in liquid nitrogen and total proteins were extracted by immunoprecipitation (IP) buffer containing 50 mM Tris–HCl (pH 7.5), 150 mM NaCl, 1 mM EDTA, 0.5% NP-40, 1 mM PMSF, and protease inhibitor cocktail (Sigma-Aldrich, St. Louis, MO, USA). After incubating the proteins (1 mg) with a monoclonal anti-GFP antibody (Abcam, Cambridge, MA, USA) and 30 μl of protein A agarose beads (Invitrogen, Carlsbad, CA, USA) at 4°C for 4 h, the precipitated complexes were washed three times with IP buffer. Proteins bound to the beads were separated on an SDS–PAGE gel and subjected to immunoblotting with anti-GFP or anti-HA antibodies. For BiFC assay, the coding regions of QSOX1, RBOHD, and GSNOR were cloned into pTOPO vector and introduced into the destination vectors, pDEST-^{GW}VYNE, pDEST-^{GW}VYCE, and pDEST-VYCE^{GW} using the LR recombination mixture (Invitrogen). After the DNA constructs were transformed into *Agrobacterium* strain GV3101, the bacteria were infiltrated into *N. benthamiana* leaves and incubated for 3 days. The fluorescence images of reconstituted YFP signals in leaves were examined under a confocal laser scanning microscope (Olympus, FV1000MPE) and analyzed by FV10-ASW 3.1 software.

Determination of the redox status of QSOX1 *in vivo*

Redox status of QSOX1 was determined *in vivo* with the procedures schematically described in Supplemental Figure 5. Protein extracts isolated from *Arabidopsis* leaves were equally divided into four aliquots. For the immunoprecipitation assay, two samples were incubated with protein A agarose immobilized with GSNOR antibody and the other two samples with protein G agarose immobilized with HA antibody for 4 h and washed three times with IP buffer. Using one of each sample type, the reduced Cys residues were labeled with 1 mM biotin-HPDP (Thermo

Fisher Scientific, Rockford, IL, USA) for 3 h in the dark at the room temperature (RT) and washed three times with PBS. For the other samples, the reduced Cys residues were blocked with 20 mM NEM for 2 h in the dark at RT followed by washing three times with PBS buffer. Then the oxidized Cys residues were reduced with 2 mM DTT for 1 h in the dark at RT followed by five washes and then labeled with 1 mM biotin-HPDP for 3 h in the dark at RT and washed three times with PBS. The proteins were separated on non-reducing SDS–PAGE gels and immunoblotted with anti-biotin, anti-HA, or anti-GSNOR antibodies.

S-Nitrosylation analysis of GSNOR and RBOHD *in vivo*

S-Nitrosylation of GSNOR and RBOHD were determined *in vivo* with the procedures schematically described in Supplemental Figure 5. Protein extracts isolated from *Arabidopsis* were immunoprecipitated with each antibody (α-GSNOR or α-RBOHD). Samples were incubated with protein A agarose immobilized with each antibody for 4 h and washed three times with IP buffer. Then the reduced Cys residues were blocked with 20 mM NEM for 2 h in the dark at RT followed by washing three times with PBS buffer. Then the S-nitrosylated Cys residues were labeled by 1 mM biotin-HPDP with 5 mM ascorbate for 3 h in the dark at RT followed by three washes with PBS. The proteins were separated on non-reducing SDS–PAGE gels and immunoblotted with anti-biotin antibody.

Measurement of GSNOR activity and SNO content

GSNOR activity was assayed spectrophotometrically at 25°C by measuring the NADH oxidation at A_{340}. After incubating leaf extracts in an assay mixture containing 20 mM Tris–HCl (pH 8.0), 0.2 mM NADH, and 0.5 mM EDTA, the reaction was started by adding GSNO at a final concentration of 400 μM. The activity was expressed as nmol-NADH consumed per min per mg of protein ($\epsilon_{340} = 6.22\ mM^{-1}\ cm^{-1}$). To measure the S-nitrosothiol (SNO) protein content, 2-week-old *Arabidopsis* seedlings grown in ½ MS media were vacuum infiltrated with bacteria and 13 plants were ground to a fine powder in a pestle with liquid nitrogen. Samples were resuspended in 1 ml of extraction buffer (1× PBS [pH 7.4]), then centrifuged at 13 500 *g* for 10 min at 4°C. The supernatant was transferred to a fresh tube and centrifuged at 16 000 *g* for 10 min at 4°C. Proteins in the supernatant were quantified by Coomassie (Bradford) protein assay kit (Thermo Fisher Scientific, Rockford, IL, USA) according to the manufacturer's instructions. The SNO content was measured by injecting 100 μl of supernatant protein fraction into the reaction vessel of Sievers' Nitric Oxide Analyzer (NOA 280i, GE Water & Process Technologies, Ratingen, Germany) containing CuCl/cysteine reducing agent as described (Yun et al., 2011) The SNO concentration determined from a standard curve generated with cySNO was divided by the protein amount to determine pmol SNO/mg protein.

NADPH oxidase activity assay

Two-week-old *Arabidopsis* seedlings grown in ½ MS media were vacuum infiltrated with bacteria and incubated for 24 h. The plants were ground to a fine powder in a pestle with liquid nitrogen. The activity of NADPH oxidase was monitored using an NADH Oxidase Activity Assay Kit (Colorimetric) (BioVision, Milpitas, CA, USA) according to the manufacturer's instructions.

Quantification and statistical analysis

Statistically significant gene expression was analyzed by Student's *t*-test (*$P < 0.05$, **$P < 0.01$), but the other statistics were performed by one-way ANOVA with Tukey's test. Samples with statistically significant difference ($P < 0.05$ or $P < 0.01$ as indicated in the figure legends) are marked with different letters (a, b, c, d, e, ab, ac), but the samples with no statistically significant difference are labeled with the same letter. "ab" is used to mark samples with no statistical difference for the two separate statistically different groups. Error bars in all of the figures represent standard deviations. Numbers of replicates are reported in the figure legends.

SUPPLEMENTAL INFORMATION

Supplemental information is available at *Molecular Plant Online*.

FUNDING

This work was supported by grants from the "BioGreen21 Agri-Tech Innovation Program (project no. PJ015824 to S.Y.L. and PJ0159992021 to M.G.K.)," Rural Development Administration (RDA), South Korea, and by the Basic Science Research Program through the National Research Foundation (NRF) of South Korea funded by the Ministry of Education (NRF-2018R1A6A3A11049525 to H.B.C.).

AUTHOR CONTRIBUTIONS

Conceptualization, H.B.C., M.G.K., D.M., and S.Y.L.; methodology, H.B.C., C.H.K., Y.H.C., S.K.P., and M.G.K.; validation, S.B.B., J.H.P., E.S.L., and S.-U.L.; investigation, H.B.C. and S.-U.L.; resources, S.D.W., B.-W.Y., W.-Y.K., and D.-J.Y.; writing – original, H.B.C., M.G.K., D.M., and S.Y.L.; writing – review & editing, H.B.C., M.G.K., D.M., and S.Y.L.; supervision, D.M. and S.Y.L.; funding acquisition, M.G.K., D.M., H.B.C., and S.Y.L.

ACKNOWLEDGMENTS

No conflict of interest declared.

Received: May 20, 2020
Revised: February 25, 2021
Accepted: May 3, 2021
Published: May 4, 2021

REFERENCES

Airaki, M., Leterrier, M., Valderrama, R., Chaki, M., Begara-Morales, J.C., Barroso, J.B., del Rio, L.A., Palma, J.M., and Corpas, F.J. (2015). Spatial and temporal regulation of the metabolism of reactive oxygen and nitrogen species during the early development of pepper (*Capsicum annuum*) seedlings. Ann. Bot. **116**:679–693.

Alejandro, S., Rodriguez, P.L., Belles, J.M., Yenush, L., Garcia-Sanchez, M.J., Fernandez, J.A., and Serrano, R. (2007). An *Arabidopsis* quiescin-sulfhydryl oxidase regulates cation homeostasis at the root symplast-xylem interface. EMBO J. **26**:3203–3215.

Alon, A., Grossman, I., Gat, Y., Kodali, V.K., DiMaio, F., Mehlman, T., Haran, G., Baker, D., Thorpe, C., and Fass, D. (2012). The dynamic disulphide relay of quiescin sulphydryl oxidase. Nature **488**:414–418.

Balmant, K.M., Zhang, T., and Chen, S. (2016). Protein phosphorylation and redox modification in stomatal guard cells. Front Physiol. **7**:26.

Begara-Morales, J.C., Sanchez-Calvo, B., Chaki, M., Valderrama, R., Mata-Perez, C., Lopez-Jaramillo, J., Padilla, M.N., Carreras, A., Corpas, F.J., and Barroso, J.B. (2014). Dual regulation of cytosolic ascorbate peroxidase (APX) by tyrosine nitration and S-nitrosylation. J. Exp. Bot. **65**:527–538.

Benayoun, B., Esnard-Feve, A., Castella, S., Courty, Y., and Esnard, F. (2001). Rat seminal vesicle FAD-dependent sulfhydryl oxidase. Biochemical characterization and molecular cloning of a member of the new sulfhydryl oxidase/quiescin Q6 gene family. J. Biol. Chem. **276**:13830–13837.

Bent, A.F., Kunkel, B.N., Dahlbeck, D., Brown, K.L., Schmidt, R., Giraudat, J., Leung, J., and Staskawicz, B.J. (1994). *RPS2* of *Arabidopsis thaliana*: a leucine-rich repeat class of plant disease resistance genes. Science **265**:1856–1860.

Chae, E., Bomblies, K., Kim, S.T., Karelina, D., Zaidem, M., Ossowski, S., Martin-Pizarro, C., Laitinen, R.A., Rowan, B.A., Tenenboim, H., et al. (2014). Species-wide genetic incompatibility analysis identifies immune genes as hot spots of deleterious epistasis. Cell **159**:1341–1351.

Chae, H.B., Moon, J.C., Shin, M.R., Chi, Y.H., Jung, Y.J., Lee, S.Y., Nawkar, G.M., Jung, H.S., Hyun, J.K., Kim, W.Y., et al. (2013).

Thioredoxin reductase type C (NTRC) orchestrates enhanced thermotolerance to *Arabidopsis* by its redox-dependent holdase chaperone function. Mol. Plant **6**:323–336.

Chugh, V., Kaur, N., and Gupta, A.K. (2011). Evaluation of oxidative stress tolerance in maize (*Zea mays* L.) seedlings in response to drought. Indian J. Biochem. Biophys. **48**:47–53.

Corpas, F.J., and Barroso, J.B. (2014). Functional implications of peroxisomal nitric oxide (NO) in plants. Front Plant Sci. **5**:97.

Corpas, F.J., Rio, L.A.D., and Palma, J.M. (2019). Impact of nitric oxide (NO) on the ROS metabolism of peroxisomes. Plants (Basel) **8**:37.

Das, P., Siegers, G.M., and Postovit, L.M. (2013). Illuminating luminal B: QSOX1 as a subtype-specific biomarker. Breast Cancer Res. **15**:104.

de Pinto, M.C., Locato, V., Sgobba, A., Romero-Puertas Mdel, C., Gadaleta, C., Delledonne, M., and De Gara, L. (2013). S-Nitrosylation of ascorbate peroxidase is part of programmed cell death signaling in tobacco bright yellow-2 cells. Plant Physiol. **163**:1766–1775.

Delledonne, M., Zeier, J., Marocco, A., and Lamb, C. (2001). Signal interactions between nitric oxide and reactive oxygen intermediates in the plant hypersensitive disease resistance response. Proc. Natl. Acad. Sci. U S A **98**:13454–13459.

Despres, C., Chubak, C., Rochon, A., Clark, R., Bethune, T., Desveaux, D., and Fobert, P.R. (2003). The *Arabidopsis* NPR1 disease resistance protein is a novel cofactor that confers redox regulation of DNA binding activity to the basic domain/leucine zipper transcription factor TGA1. Plant Cell **15**:2181–2191.

Ding, Y., Sun, T., Ao, K., Peng, Y., Zhang, Y., Li, X., and Zhang, Y. (2018). Opposite roles of salicylic acid receptors NPR1 and NPR3/NPR4 in transcriptional regulation of plant immunity. Cell **173**:1454–1467.e15.

Dubiella, U., Seybold, H., Durian, G., Komander, E., Lassig, R., Witte, C.P., Schulze, W.X., and Romeis, T. (2013). Calcium-dependent protein kinase/NADPH oxidase activation circuit is required for rapid defense signal propagation. Proc. Natl. Acad. Sci. U S A **110**:8744–8749.

El-Maarouf-Bouteau, H., and Bailly, C. (2008). Oxidative signaling in seed germination and dormancy. Plant Signal Behav. **3**:175–182.

Farmer, E.E., and Mueller, M.J. (2013). ROS-mediated lipid peroxidation and RES-activated signaling. Annu. Rev. Plant Biol. **64**:429–450.

Feechan, A., Kwon, E., Yun, B.W., Wang, Y., Pallas, J.A., and Loake, G.J. (2005). A central role for S-nitrosothiols in plant disease resistance. Proc. Natl. Acad. Sci. U S A **102**:8054–8059.

Foreman, J., Demidchik, V., Bothwell, J.H., Mylona, P., Miedema, H., Torres, M.A., Linstead, P., Costa, S., Brownlee, C., Jones, J.D., et al. (2003). Reactive oxygen species produced by NADPH oxidase regulate plant cell growth. Nature **422**:442–446.

Foyer, C.H., and Noctor, G. (2005). Redox homeostasis and antioxidant signaling: a metabolic interface between stress perception and physiological responses. Plant Cell **17**:1866–1875.

Frederickson Matika, D.E., and Loake, G.J. (2014). Redox regulation in plant immune function. Antioxid. Redox Signal. **21**:1373–1388.

Garcia-Santamarina, S., Boronat, S., and Hidalgo, E. (2014). Reversible cysteine oxidation in hydrogen peroxide sensing and signal transduction. Biochemistry **53**:2560–2580.

Gomez-Gomez, L., and Boller, T. (2000). FLS2: an LRR receptor-like kinase involved in the perception of the bacterial elicitor flagellin in *Arabidopsis*. Mol. Cell **5**:1003–1011.

Grant, J.J., and Loake, G.J. (2000). Role of reactive oxygen intermediates and cognate redox signaling in disease. Plant Physiol. **124**:21–29.

Grant, M.R., Godiard, L., Straube, E., Ashfield, T., Lewald, J., Sattler, A., Innes, R.W., and Dangl, J.L. (1995). Structure of the *Arabidopsis RPM1* gene enabling dual specificity disease resistance. Science **269**:843–846.

Halane, M.K., Kim, S.H., Spears, B.J., Garner, C.M., Rogan, C.J., Okafor, E.C., Su, J., Bhattacharjee, S., and Gassmann, W. (2018). The bacterial type III-secreted protein AvrRps4 is a bipartite effector. Plos Pathog. **14**:e1006984.

Herrera-Vasquez, A., Salinas, P., and Holuigue, L. (2015). Salicylic acid and reactive oxygen species interplay in the transcriptional control of defense genes expression. Front Plant Sci. **6**:171.

Hillion, M., and Antelmann, H. (2015). Thiol-based redox switches in prokaryotes. Biol. Chem. **396**:415–444.

Huh, S.U., Cevik, V., Ding, P., Duxbury, Z., Ma, Y., Tomlinson, L., Sarris, P.F., and Jones, J.D.G. (2017). Protein-protein interactions in the RPS4/RRS1 immune receptor complex. PLoS Pathog. **13**:e1006376.

Ilani, T., Alon, A., Grossman, I., Horowitz, B., Kartvelishvily, E., Cohen, S.R., and Fass, D. (2013). A secreted disulfide catalyst controls extracellular matrix composition and function. Science **341**:74–76.

Jang, H.H., Lee, K.O., Chi, Y.H., Jung, B.G., Park, S.K., Park, J.H., Lee, J.R., Lee, S.S., Moon, J.C., Yun, J.W., et al. (2004). Two enzymes in one; two yeast peroxiredoxins display oxidative stress-dependent switching from a peroxidase to a molecular chaperone function. Cell **117**:625–635.

Jin, L., and Mackey, D.M. (2017). Measuring callose deposition, an indicator of cell wall reinforcement, during bacterial infection in *Arabidopsis*. Methods Mol. Biol. **1578**:195–205.

Jones, J.D., and Dangl, J.L. (2006). The plant immune system. Nature **444**:323–329.

Jwa, N.S., and Hwang, B.K. (2017). Convergent evolution of pathogen effectors toward reactive oxygen species signaling networks in plants. Front Plant Sci. **8**:1687.

Kadota, Y., Shirasu, K., and Zipfel, C. (2015). Regulation of the NADPH oxidase RBOHD during plant immunity. Plant Cell Physiol. **56**:1472–1480.

Katchman, B.A., Antwi, K., Hostetter, G., Demeure, M.J., Watanabe, A., Decker, G.A., Miller, L.J., Von Hoff, D.D., and Lake, D.F. (2011). Quiescin sulfhydryl oxidase 1 promotes invasion of pancreatic tumor cells mediated by matrix metalloproteinases. Mol. Cancer Res. **9**:1621–1631.

Kovacs, I., Durner, J., and Lindermayr, C. (2015). Crosstalk between nitric oxide and glutathione is required for NONEXPRESSOR OF PATHOGENESIS-RELATED GENES 1 (NPR1)-dependent defense signaling in *Arabidopsis thaliana*. New Phytol. **208**:860–872.

Kunkel, B.N., Bent, A.F., Dahlbeck, D., Innes, R.W., and Staskawicz, B.J. (1993). RPS2, an *Arabidopsis* disease resistance locus specifying recognition of *Pseudomonas syringae* strains expressing the avirulence gene avrRpt2. Plant Cell **5**:865–875.

Kwak, J.M., Mori, I.C., Pei, Z.M., Leonhardt, N., Torres, M.A., Dangl, J.L., Bloom, R.E., Bodde, S., Jones, J.D., and Schroeder, J.I. (2003). NADPH oxidase AtrbohD and AtrbohF genes function in ROS-dependent ABA signaling in *Arabidopsis*. EMBO J. **22**:2623–2633.

Leon-Reyes, A., Van der Does, D., De Lange, E.S., Delker, C., Wasternack, C., Van Wees, S.C., Ritsema, T., and Pieterse, C.M. (2010). Salicylate-mediated suppression of jasmonate-responsive gene expression in *Arabidopsis* is targeted downstream of the jasmonate biosynthesis pathway. Planta **232**:1423–1432.

Lightfoot, D.J., McGrann, G.R., and Able, A.J. (2017). The role of a cytosolic superoxide dismutase in barley-pathogen interactions. Mol. Plant Pathol. **18**:323–335.

Limor-Waisberg, K., Alon, A., Mehlman, T., and Fass, D. (2012). Phylogenetics and enzymology of plant quiescin sulfhydryl oxidase. FEBS Lett. **586**:4119–4125.

Lindermayr, C., Sell, S., Muller, B., Leister, D., and Durner, J. (2010). Redox regulation of the NPR1-TGA1 system of *Arabidopsis thaliana* by nitric oxide. Plant Cell **22**:2894–2907.

Liu, Y., and He, C. (2016). Regulation of plant reactive oxygen species (ROS) in stress responses: learning from AtRBOHD. Plant Cell Rep. **35**:995–1007.

Loon, V.L.C., and Strien, V.E.A. (1999). The families of pathogenesis-related proteins, their activities, and comparative analysis of PR-1 type proteins. Physiol. Mol. Plant Pathol. **55**:85–97.

Malik, S.I., Hussain, A., Yun, B.W., Spoel, S.H., and Loake, G.J. (2011). GSNOR-mediated de-nitrosylation in the plant defence response. Plant Sci. **181**:540–544.

Margittai, E., and Sitia, R. (2011). Oxidative protein folding in the secretory pathway and redox signaling across compartments and cells. Traffic **12**:1–8.

Marino, D., Dunand, C., Puppo, A., and Pauly, N. (2012). A burst of plant NADPH oxidases. Trends Plant Sci. **17**:9–15.

Mateo, A., Funck, D., Muhlenbock, P., Kular, B., Mullineaux, P.M., and Karpinski, S. (2006). Controlled levels of salicylic acid are required for optimal photosynthesis and redox homeostasis. J. Exp. Bot. **57**:1795–1807.

Miller, G., Schlauch, K., Tam, R., Cortes, D., Torres, M.A., Shulaev, V., Dangl, J.L., and Mittler, R. (2009). The plant NADPH oxidase RBOHD mediates rapid systemic signaling in response to diverse stimuli. Sci. Signal. **2**:ra45.

Mindrinos, M., Katagiri, F., Yu, G.-L., and Ausubel, F.M. (1994). The *A. thaliana* disease resistance gene *RPS2* encodes a protein containing a nucleotide-binding site and leucine-rich repeats. Cell **78**:1089–1099.

Mou, Z., Fan, W., and Dong, X. (2003). Inducers of plant systemic acquired resistance regulate NPR1 function through redox changes. Cell **113**:935–944.

Mur, L.A., Kenton, P., Atzorn, R., Miersch, O., and Wasternack, C. (2006). The outcomes of concentration-specific interactions between salicylate and jasmonate signaling include synergy, antagonism, and oxidative stress leading to cell death. Plant Physiol. **140**:249–262.

Narusaka, M., Shirasu, K., Noutoshi, Y., Kubo, Y., Shiraishi, T., Iwabuchi, M., and Narusaka, Y. (2009). RRS1 and RPS4 provide a dual resistance-gene system against fungal and bacterial pathogens. Plant J. **60**:218–226.

Oda, T., Hashimoto, H., Kuwabara, N., Akashi, S., Hayashi, K., Kojima, C., Wong, H.L., Kawasaki, T., Shimamoto, K., Sato, M., et al. (2010). Structure of the N-terminal regulatory domain of a plant NADPH oxidase and its functional implications. J. Biol. Chem. **285**:1435–1445.

Okuda, A., Matsusaki, M., Higashino, Y., Masuda, T., and Urade, R. (2014). Disulfide bond formation activity of soybean quiescin sulfhydryl oxidase. FEBS J. **281**:5341–5355.

Ortega-Galisteo, A.P., Rodriguez-Serrano, M., Pazmino, D.M., Gupta, D.K., Sandalio, L.M., and Romero-Puertas, M.C. (2012). S-Nitrosylated proteins in pea (*Pisum sativum* L.) leaf peroxisomes: changes under abiotic stress. J. Exp. Bot. **63**:2089–2103.

Ostman, A., Frijhoff, J., Sandin, A., and Bohmer, F.D. (2011). Regulation of protein tyrosine phosphatases by reversible oxidation. J. Biochem. **150**:345–356.

Pauly, N., Pucciariello, C., Mandon, K., Innocenti, G., Jamet, A., Baudouin, E., Herouart, D., Frendo, P., and Puppo, A. (2006). Reactive oxygen and nitrogen species and glutathione: key players in the legume-*Rhizobium* symbiosis. J. Exp. Bot. **57**:1769–1776.

Pernodet, N., Hermetet, F., Adami, P., Vejux, A., Descotes, F., Borg, C., Adams, M., Pallandre, J.R., Viennet, G., Esnard, F., et al. (2012). High expression of QSOX1 reduces tumorogenesis, and is associated with a better outcome for breast cancer patients. Breast Cancer Res. **14**:R136.

Pogany, M., von Rad, U., Grun, S., Dongo, A., Pintye, A., Simoneau, P., Bahnweg, G., Kiss, L., Barna, B., and Durner, J. (2009). Dual roles of reactive oxygen species and NADPH oxidase RBOHD in an *Arabidopsis-Alternaria* pathosystem. Plant Physiol. **151**:1459–1475.

Poillet, L., Pernodet, N., Boyer-Guittaut, M., Adami, P., Borg, C., Jouvenot, M., Delage-Mourroux, R., and Despouy, G. (2014). QSOX1 inhibits autophagic flux in breast cancer cells. PLoS One **9**:e86641.

Qi, G., Chen, J., Chang, M., Chen, H., Hall, K., Korin, J., Liu, F., Wang, D., and Fu, Z.Q. (2018). Pandemonium breaks out: disruption of salicylic acid-mediated defense by plant pathogens. Mol. Plant **11**:1427–1439.

Romero-Puertas, M.C., Laxa, M., Matte, A., Zaninotto, F., Finkemeier, I., Jones, A.M., Perazzolli, M., Vandelle, E., Dietz, K.J., and Delledonne, M. (2007). S-nitrosylation of peroxiredoxin II E promotes peroxynitrite-mediated tyrosine nitration. Plant Cell **19**:4120–4130.

Sakaguchi, S., Yamaguchi, T., Nomura, T., and Ono, M. (2008). Regulatory T cells and immune tolerance. Cell **133**:775–787.

Schwessinger, B., and Ronald, P.C. (2012). Plant innate immunity: perception of conserved microbial signatures. Annu. Rev. Plant Biol. **63**:451–482.

Shi, C.Y., Fan, Y., Liu, B., and Lou, W.H. (2013). HIF1 contributes to hypoxia-induced pancreatic cancer cells invasion via promoting QSOX1 expression. Cell Physiol. Biochem. **32**:561–568.

Spadaro, D., Yun, B.W., Spoel, S.H., Chu, C., Wang, Y.Q., and Loake, G.J. (2010). The redox switch: dynamic regulation of protein function by cysteine modifications. Physiol. Plant **138**:360–371.

Tada, Y., Spoel, S.H., Pajerowska-Mukhtar, K., Mou, Z., Song, J., Wang, C., Zuo, J., and Dong, X. (2008). Plant immunity requires conformational changes [corrected] of NPR1 via S-nitrosylation and thioredoxins. Science **321**:952–956.

Thorpe, C., Hoober, K.L., Raje, S., Glynn, N.M., Burnside, J., Turi, G.K., and Coppock, D.L. (2002). Sulfhydryl oxidases: emerging catalysts of protein disulfide bond formation in eukaryotes. Arch. Biochem. Biophys. **405**:1–12.

Todesco, M., Balasubramanian, S., Hu, T.T., Traw, M.B., Horton, M., Epple, P., Kuhns, C., Sureshkumar, S., Schwartz, C., Lanz, C., et al. (2010). Natural allelic variation underlying a major fitness trade-off in *Arabidopsis thaliana*. Nature **465**:632–636.

Torres, M.A. (2010). ROS in biotic interactions. Physiol. Plant **138**:414–429.

Torres, M.A., and Dangl, J.L. (2005). Functions of the respiratory burst oxidase in biotic interactions, abiotic stress and development. Curr. Opin. Plant Biol. **8**:397–403.

Torres, M.A., Dangl, J.L., and Jones, J.D. (2002). *Arabidopsis* gp91phox homologues AtrbohD and AtrbohF are required for accumulation of reactive oxygen intermediates in the plant defense response. Proc. Natl. Acad. Sci. U S A **99**:517–522.

Trachootham, D., Alexandre, J., and Huang, P. (2009). Targeting cancer cells by ROS-mediated mechanisms: a radical therapeutic approach? Nat. Rev. Drug Discov. **8**:579–591.

Tristan, C., Shahani, N., Sedlak, T.W., and Sawa, A. (2011). The diverse functions of GAPDH: views from different subcellular compartments. Cell Signal. **23**:317–323.

Tsuda, K., and Katagiri, F. (2010). Comparing signaling mechanisms engaged in pattern-triggered and effector-triggered immunity. Curr. Opin. Plant Biol. **13**:459–465.

Tu, B.P., Ho-Schleyer, S.C., Travers, K.J., and Weissman, J.S. (2000). Biochemical basis of oxidative protein folding in the endoplasmic reticulum. Science **290**:1571–1574.

Turkan, I. (2018). ROS and RNS: key signalling molecules in plants. J. Exp. Bot. **69**:3313–3315.

Vandelle, E., Ling, T., Imanifard, Z., Liu, R., Delledonne, M., and Bellin, D. (2016). Chapter eleven—Nitric oxide signaling during the hypersensitive disease resistance response. Adv. Bot. Res. **77**:219–243.

Vazquez-Torres, A. (2012). Redox active thiol sensors of oxidative and nitrosative stress. Antioxid. Redox Signal. **17**:1201–1214.

Veal, E.A., Day, A.M., and Morgan, B.A. (2007). Hydrogen peroxide sensing and signaling. Mol. Cell **26**:1–14.

Wang, P., Du, Y., Hou, Y.J., Zhao, Y., Hsu, C.C., Yuan, F., Zhu, X., Tao, W.A., Song, C.P., and Zhu, J.K. (2015a). Nitric oxide negatively regulates abscisic acid signaling in guard cells by S-nitrosylation of OST1. Proc. Natl. Acad. Sci. U S A **112**:613–618.

Wang, P., Zhu, J.K., and Lang, Z. (2015b). Nitric oxide suppresses the inhibitory effect of abscisic acid on seed germination by S-nitrosylation of SnRK2 proteins. Plant Signal Behav. **10**:e1031939.

Wang, W., Xia, M.X., Chen, J., Yuan, R., Deng, F.N., and Shen, F.F. (2016). Gene expression characteristics and regulation mechanisms of superoxide dismutase and its physiological roles in plants under stress. Biochemistry (Mosc) **81**:465–480.

Weerapana, E., Wang, C., Simon, G.M., Richter, F., Khare, S., Dillon, M.B., Bachovchin, D.A., Mowen, K., Baker, D., and Cravatt, B.F. (2010). Quantitative reactivity profiling predicts functional cysteines in proteomes. Nature **468**:790–795.

Wildermuth, M.C., Dewdney, J., Wu, G., and Ausubel, F.M. (2001). Isochorismate synthase is required to synthesize salicylic acid for plant defence. Nature **414**:562–565.

Wiseman, H., and Halliwell, B. (1996). Damage to DNA by reactive oxygen and nitrogen species: role in inflammatory disease and progression to cancer. Biochem. J. **313** (Pt 1):17–29.

Xu, S., Guerra, D., Lee, U., and Vierling, E. (2013). S-Nitrosoglutathione reductases are low-copy number, cysteine-rich proteins in plants that control multiple developmental and defense responses in *Arabidopsis*. Front Plant Sci. **4**:430.

Yang, H., Mu, J., Chen, L., Feng, J., Hu, J., Li, L., Zhou, J.M., and Zuo, J. (2015). S-Nitrosylation positively regulates ascorbate peroxidase activity during plant stress responses. Plant Physiol. **167**:1604–1615.

Yun, B.W., Feechan, A., Yin, M., Saidi, N.B., Le Bihan, T., Yu, M., Moore, J.W., Kang, J.G., Kwon, E., Spoel, S.H., et al. (2011). S-Nitrosylation of NADPH oxidase regulates cell death in plant immunity. Nature **478**:264–268.

Zhang, Y., Dorey, S., Swiderski, M., and Jones, J.D. (2004). Expression of RPS4 in tobacco induces an AvrRps4-independent HR that requires EDS1, SGT1 and HSP90. Plant J. **40**:213–224.

Zhou, S., Jia, L., Chu, H., Wu, D., Peng, X., Liu, X., Zhang, J., Zhao, J., Chen, K., and Zhao, L. (2016). *Arabidopsis* CaM1 and CaM4 promote nitric oxide production and salt resistance by inhibiting S-nitrosoglutathione reductase via direct binding. PLoS Genet. **12**:e1006255.

Zhu, W., Zaidem, M., Van de Weyer, A.L., Gutaker, R.M., Chae, E., Kim, S.T., Bemm, F., Li, L., Todesco, M., Schwab, R., et al. (2018). Modulation of ACD6 dependent hyperimmunity by natural alleles of an *Arabidopsis thaliana* NLR resistance gene. PLoS Genet. **14**:e1007628.

Zipfel, C. (2014). Plant pattern-recognition receptors. Trends Immunol. **35**:345–351.